

Second Generation Tetrahydroquinoline-Based Protein Farnesyltransferase Inhibitors as Antimalarials

Pravin Bendale,[†] Srinivas Olepu,[†] Praveen Kumar Suryadevara,[†] Vivek Bulbule,[†] Kasey Rivas,^{‡,§} Laxman Nallan,[†] Brian Smart,[†] Kohei Yokoyama,[†] Sudha Ankala,[†] Prakash Rao Pendyala,^{||} David Floyd,[⊥] Louis J. Lombardo,[#] David K. Williams,[#] Frederick S. Buckner,^{‡,§} Debopam Chakrabarti,^{||} Christophe L. M. J. Verlinde,[◇] Wesley C. Van Voorhis,^{‡,§} and Michael H. Gelb^{*,†,◇}

Departments of Chemistry, Medicine, Pathobiology, and Biochemistry, University of Washington, Seattle, Washington 98195, Department of Molecular Biology and Microbiology, University of Central Florida, Orlando, Florida 32826, Pharmacopeia Drug Discovery, Princeton, New Jersey, and Bristol-Myers Squibb Pharmaceutical Research Institute, Princeton, New Jersey 08543-4000

Received March 22, 2007

Substituted tetrahydroquinolines (THQs) have been previously identified as inhibitors of mammalian protein farnesyltransferase (PFT). Previously we showed that blocking PFT in the malaria parasite led to cell death and that THQ-based inhibitors are the most potent among several structural classes of PFT inhibitors (PFTIs). We have prepared 266 THQ-based PFTIs and discovered several compounds that inhibit the malarial enzyme in the sub- to low-nanomolar range and that block the growth of the parasite (*P. falciparum*) in the low-nanomolar range. This body of structure–activity data can be rationalized in most cases by consideration of the X-ray structure of one of the THQs bound to mammalian PFT together with a homology structural model of the malarial enzyme. The results of this study provide the basis for selection of antimalarial PFTIs for further evaluation in preclinical drug discovery assays.

Introduction

New antimalarial drugs are needed because of widespread resistance to well-established agents such as chloroquine (www.mmv.org). We have been working on inhibitors of malaria protein farnesyltransferase (PFT^a) because earlier studies showed that such agents are cytotoxic to *Plasmodium falciparum*,^{1–3} the causative agent of falciparum malaria. PFT catalyzes the transfer of the 15-carbon farnesyl group from farnesyl-pyrophosphate to the SH group of the tetrapeptide motif CaaX (C is cysteine, a is usually but not necessarily an aliphatic amino acid, and X is a variety of amino acids) present at the C-terminus of proteins that become farnesylated. Inhibitors of mammalian PFT have been extensively developed as anticancer agents by the pharmaceutical industry,⁴ and thus, we have the opportunity to extend the medicinal chemistry and preclinical pharmacology of PFT inhibitors toward the development of antimalarial drugs (piggy-back drug development). To this end, we tested many of the known classes of PFT inhibitors and found that tetrahydroquinoline (THQ)-based PFT inhibitors developed at Bristol Myers Squibb⁵ are the most potent against *P. falciparum* PFT (Pf-PFT) and against parasite growth in human red blood cells.³ Our previous medicinal chemistry efforts led to the identification of THQ **1** (Figure 1) and a few related compounds that inhibit Pf-PFT in vitro, with IC₅₀ (concentration of inhibitor that 50% inhibits Pf-PFT) values of ~0.6 nM, and inhibit parasite growth in red cells with ED₅₀ (concentration of inhibitor that 50%

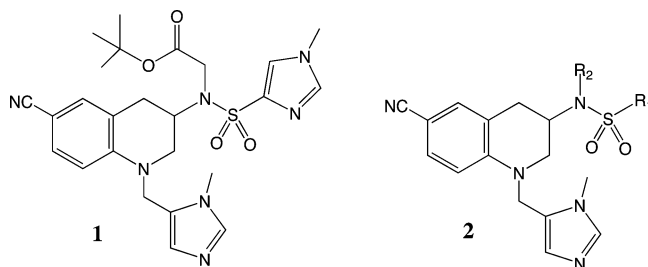


Figure 1. Tetrahydroquinoline-based protein farnesyltransferase inhibitors. See main text for discussion.

inhibits the growth of *P. falciparum* in red blood cells in vitro) values of ~5 nM.³ Studies with mammalian PFT have shown that the 6-cyano group on the THQ ring is important in conferring tight enzyme binding,⁶ and structural studies show that the imidazole appended to N-1 of the THQ ring directly coordinates the Zn²⁺ ion at the active site of mammalian PFT.^{7,8}

Continuous dosing of THQ **1** using surgically implanted, osmotic minipumps in mice infected with rodent malaria (*P. berghei*) led to a dramatic reduction in parasite number.³ Studies of malaria resistance to these Pf-PFT inhibitors provided very strong evidence that blocking Pf-PFT action is the basis for parasite killing.^{7,8} The reasons that PFT inhibitors are very toxic to malarial cells but not to mammalian cells are not known. One hypothesis is that the malaria parasite appears to lack protein geranylgeranyltransferase type I, the enzyme responsible for the monogeranylgeranylation of proteins in mammalian cells. Thus, some critical housekeeping proteins may be farnesylated in malaria but geranylgeranylated in mammalian cells.

The purpose of the present study is to report our continued efforts to develop THQ-based antimalarials. A number of THQs were prepared with various groups attached to the sulfonyl group of **1** (R₁ of THQ **1** in Figure 1) or to the sulfonamide nitrogen (R₂ in THQ **2** in Figure 1). Less extensive structure–activity studies were carried out by variation of other groups attached to the THQ core. We were able to identify several new THQ-based Pf-PFT inhibitors with sub- to low-nanomolar potency

* To whom correspondence should be addressed. Phone: 206-543-7142. Fax: 206-685-8665. E-mail: gelb@chem.washington.edu.

[†] Department of Chemistry, University of Washington.

[‡] Department of Medicine, University of Washington.

[§] Department of Pathobiology, University of Washington.

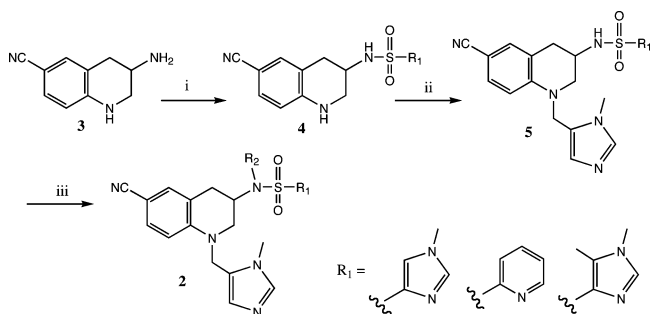
^{||} Department of Molecular Biology and Microbiology, University of Central Florida.

[⊥] Pharmacopeia Drug Discovery.

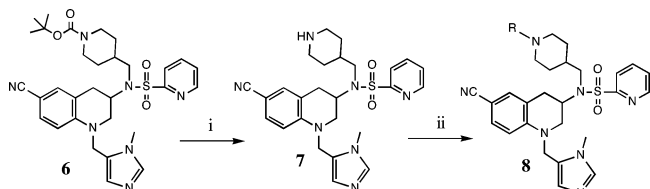
[#] Bristol-Myers Squibb Pharmaceutical Research Institute.

[◇] Department of Biochemistry, University of Washington.

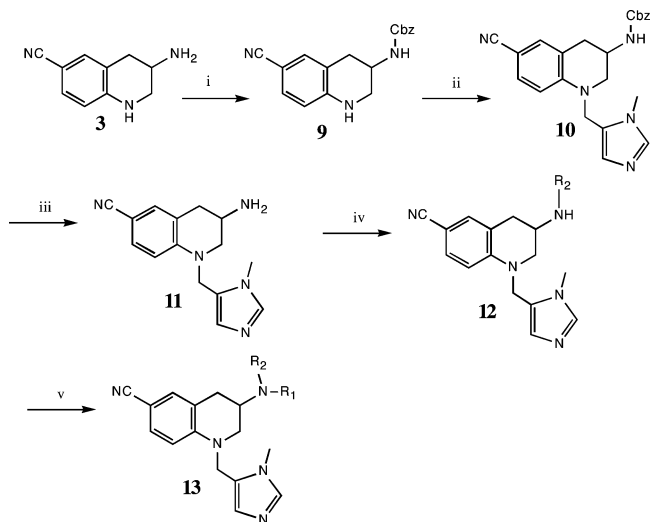
^a Abbreviations: ED₅₀, effective dose of inhibitor that reduces parasite growth in vitro by 50%; IC₅₀, inhibitor concentration that reduces the rate of PFT in vitro by 50%; PFT, protein farnesyltransferase; PFTI, PFT inhibitor; THQ, tetrahydroquinoline.

Scheme 1^a

^a Reagents and conditions: (i) R_1SO_2Cl , DIPEA, CH_3CN ; (ii) 1-methyl-1*H*-imidazole-5-carboxaldehyde, triethylsilane, 1,2-dichloroethane:trifluoroacetic acid (1:1); (iii) R_2-Br , Cs_2CO_3 , DMF.

Scheme 2^a

^a Reagents and conditions: (i) 10% trifluoroacetic acid, CH_2Cl_2 ; (ii) $ROCOCl$ or $ROCOCl$ or $RNCO$ or RSO_2Cl , CH_2Cl_2 , DIPEA.

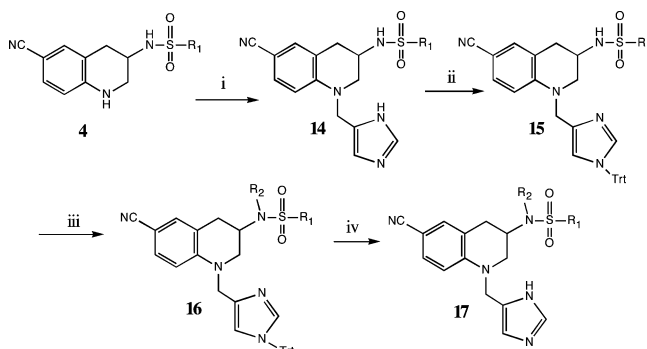
Scheme 3^a

^a Reagents and conditions: (i) $Cbz-Cl$, Et_3N , CH_3CN ; (ii) 1-methyl-1*H*-imidazole-5-carboxaldehyde, triethylsilane, 1,2-dichloroethane:trifluoroacetic acid (1:1); (iii) 10% Pd/C , CH_3OH ; (iv) R_2-Br , Cs_2CO_3 , DMF; (v) R_1COOH , EDC, $HOBt$, Et_3N , DMF, or R_1COCl , Et_3N , CH_2Cl_2 or R_1SO_2Cl , Et_3N , CH_2Cl_2 .

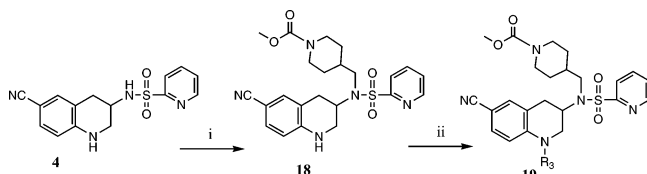
on Pf-PFT and with low nanomolar potency on *P. falciparum* growth in vitro.

Chemistry

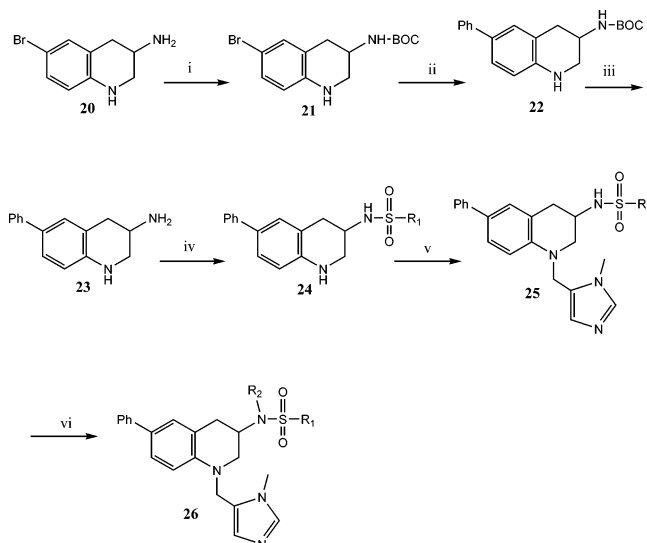
Many of the THQs **2** prepared in this study were prepared by the route shown in Scheme 1 starting from racemic 6-cyano-3-amino-THQ (compound **3**, Scheme 1), which was made as described.⁵ This route is useful for variation of the R_2 group, which is added in the last synthetic step. Scheme 2 was used to prepare analogs of **2** in which the R group attached to the piperidine nitrogen is varied. Scheme 3 was used to allow easier variation of both the R_1 and R_2 groups because, unlike in Scheme 1, the R_1 group is introduced later in the synthesis. Scheme 4 was used to prepare THQs, which lack the methyl

Scheme 4^a

^a Reagents and conditions: (i) 3*H*-imidazole-4-carboxaldehyde, triethylsilane, 1,2-dichloroethane/trifluoroacetic acid (1:1); (ii) trityl chloride, DIPEA, DMF; (iii) R_2-Br , Cs_2CO_3 , DMF; (iv) CH_2Cl_2 , trifluoroacetic acid.

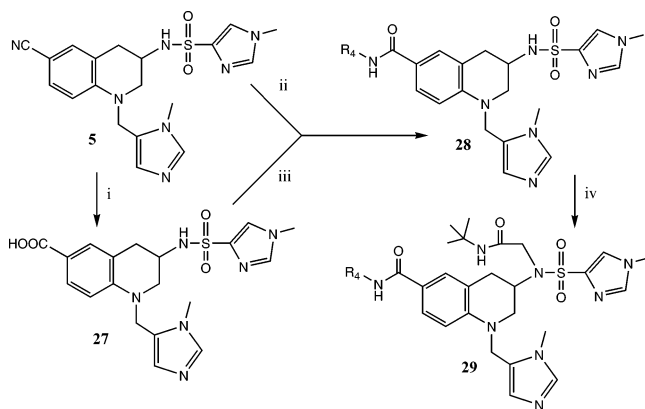
Scheme 5^a

^a Reagents and conditions: (i) R_2-Br , Cs_2CO_3 , DMF; (ii) 3-methyl-3*H*-imidazole-4-sulfonyl chloride, DMAP, CH_3CN .

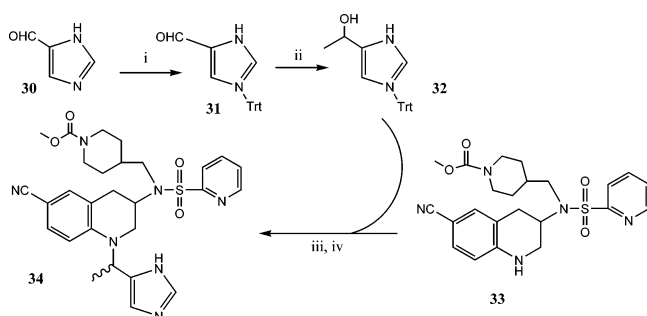
Scheme 6^a

^a Reagents and conditions: (i) BOC-anhydride, K_2CO_3 , dioxane-water (4:1); (ii) phenylboronic acid, $Ba(OH)_2$, tetrakis triphenylphosphine palladium, DME-water (5:1); (iii) 20% trifluoroacetic acid, CH_2Cl_2 ; (iv) R_1SO_2Cl , DIPEA, CH_2Cl_2 ; (v) 1-methyl-1*H*-imidazole-5-carboxaldehyde, triethylsilane, 1,2-dichloroethane/trifluoroacetic acid (1:1); (vi) R_2-Br , Cs_2CO_3 , DMF.

group on the zinc-binding imidazole. In this case, tritylation of the imidazole was required prior to alkylation of the sulfonamide nitrogen. Scheme 5 shows the synthesis of a THQ analog in which the methylene bridge between the N-1 of the THQ core and the Zn^{2+} -binding imidazole group is replaced with a sulfonyl group or with a $CH(CH_3)$ group. THQs containing a 6-phenyl group in place of the 6-cyano group were prepared according to Scheme 6. The key step is the introduction of the phenyl group via Suzuki coupling (conversion of **21** to **22**). Scheme 7 shows the synthesis of THQ analogs in which the 6-CN is replaced with carbonyl-bearing functional groups. Scheme 8 was used to prepare the THQ analog **34**. The key reaction is

Scheme 7^a

^a Reagents and conditions: (i) concd HCl, 80 °C; (ii) H₂SO₄, R₄-OH; (iii) R₄-NH₂, EDC, DMAP, DMF; (iv) alkyl bromide, Cs₂CO₃, DMF.

Scheme 8^a

^a Reagents and conditions: (i) trityl chloride, Et₃N, DMF; (ii) MeMgBr, THF, 0 °C; (iii) MsCl, CH₃CN, 60 °C; (iv) trifluoroacetic acid, CH₂Cl₂.

nucleophilic displacement between the mesylate derived from the indicated secondary alcohol **32** and secondary amine **33**.

Inhibition of Pf-PFT and *P. falciparum* Growth by THQ-Based Pf-PFT Inhibitors. We first give a general description of the potencies of THQ-based Pf-PFT inhibitors on the enzyme and on *P. falciparum* growth *in vitro*, and then we attempt to provide a structural rationale for some of the activity data. Our initial structure–activity data on THQ-based inhibitors of Pf-PFT led to the discovery of compounds with R₁ = 2-pyridyl or N₁-methyl-4-imidazolyl as being potent inhibitors of Pf-PFT.³ In Table 1, we report a study of THQs with R₁ = 2-pyridyl and with a variety of substituents as R₂ groups. A number of THQs were found that inhibited Pf-PFT *in vitro* by 50% (IC₅₀) in the low nanomolar range and that also inhibited the growth of *P. falciparum* in erythrocyte cultures *in vitro* by 50% (ED₅₀) in the low nanomolar range (i.e., **48**, **55**, **56**, **57**, **61**, and **62**). The most potent compound in the series is **55** with an ED₅₀ = 17 nM for the 3D7 strain and 10 nM for the K1 strain. Well-established antimalarial drugs such as chloroquine display ED₅₀ values in the low nanomolar range. Thus, the potency achieved for some of our THQ-based PFT inhibitors is probably sufficient for an antimalarial drug discovery effort. In general, we did not find any compound that inhibited *P. falciparum* growth in the low nanomolar range that was a relatively poor inhibitor of Pf-PFT.

Table 2 summarizes results for THQ-based PFT inhibitors with R₁ = N₁-methyl-4-imidazolyl and with variation of the R₂ group. Many compounds were found with IC₅₀s and ED₅₀s in the low nanomolar range. The most potent in the series are **106**, **107**, **102**, **104**, **115**, and **131** with values of ED₅₀ < 10

nM. Compound **106** shows exceptional potency with an ED₅₀ = 1.8 nM. This is the most potent compound in terms of ED₅₀ that we found in the current study and among the most potent antimalarials ever reported. In general, the compounds with R₁ = N₁-methyl-4-imidazolyl are more potent than the analogous compounds with R₁ = 2-pyridyl.

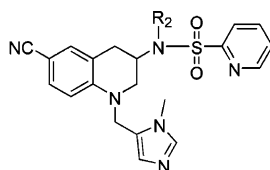
We also carried out side-by-side pharmacokinetic studies of potent THQ-based Pf-PFT inhibitors to discover a compound that could be tested in malaria-infected rodents.⁹ We measured the rate of flux of THQ-based PFT inhibitors across a tight-junction monolayer of Caco-2 cells and showed that this *in vitro* assay is a good predictor of oral bioavailability of these compounds in rodents.⁹ In general, we found that R₁ = 2-pyridyl promotes better Caco-2 permeability and oral bioavailability than compounds with R₁ = N₁-methyl-4-imidazolyl.⁹ Because it appears that THQ-based PFT inhibitors are cleared in rodents by hepatic metabolism, we measured the half-time for metabolism of THQs by rat and mouse liver microsomes *in vitro*.⁹ Based on an overall balance of desirable properties, **6** emerged as a promising antimalarial lead compound.⁹ Thus, we investigated in detail the structure–activity relationships among **6** analogs. Table 3 shows the results with **6** analogs in which the R group attached to the piperidine N of the R₂ group is varied. In general, we found a good correlation between IC₅₀ values for Pf-PFT inhibition and ED₅₀ values for blocking the growth of parasites *in vitro*.

When those compounds in Table 3 with values of ED₅₀ < ~100 nM were tested for Caco-2 permeability and microsomal stability,⁹ **162** emerged as a compound with a good balance of potency and desirable pharmacokinetic properties. In Table 4, we summarize results with compounds in which R₂ is held as the R₂ of **162** and R₁ is varied. We also studied compounds with R₂ = 2-fluorophenylCH₂, 4-MeSO₂-phenylCH₂, and *t*-BuNHCOCH₂ because these groups led to potent compounds in the early scans. Most compounds in this series were significantly less potent on Pf-PFT and on parasites compared to **162**. The exceptions were those with a small heterocyclic R₁ group, that is, **191**.

Molecular modeling studies described below suggested that addition of a Me group to R₁ = N₁-methyl-4-imidazolyl at the 5-position would better fill the R₁-binding pocket on Pf-PFT. Table 5 shows a scan of R₂ groups keeping R₁ as 4-(N₁-methyl-5-Me-imidazolyl). Compound **234** with the same R₂ as in **162** emerged as the best compound.

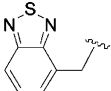
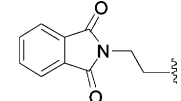
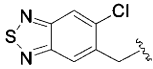
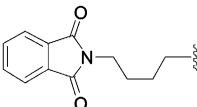
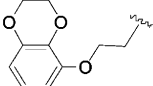
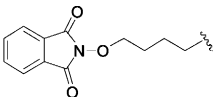
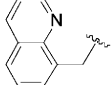
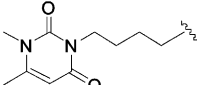
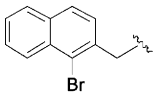
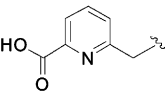
Table 6 gives the activity of compounds in which the sulfonyl is replaced by carbonyl (sulfonamide to amide change). In general, these compounds are much poorer inhibitors of Pf-PFT and of *P. falciparum* growth than the corresponding sulfonyl-containing THQ compounds. Thus, we prepared only a limited set of these amide-containing THQ compounds.

Table 7 shows THQ-based compounds with alteration to the *N*-Me-imidazoleCH₂ group attached to the THQ ring N. This substituted imidazole is a direct ligand to the Zn²⁺ at the active site of Pf-PFT (see below). Removal of the Me group from the imidazole has only a minimal effect on binding to Pf-PFT (as predicted by modeling) but greatly increases ED₅₀ for killing parasites, suggesting that methylation of the Zn²⁺-binding imidazole promotes penetration of compound across erythrocyte and parasite membranes. Replacement of the CH₂ that links the imidazole to the THQ ring N by SO₂ obliterates binding to Pf-PFT and antiparasite activity. Addition of a Me group to this CH₂ bridge (mixture of four stereoisomers) also greatly reduces activity as does replacement of the imidazole by a 3-pyridylCH₂ group.

Table 1. 6-CN-THQs with R₁ = 2-Pyridyl^a

Compound	R ₂	PfPFT % Inhibition at			ED ₅₀ (nM)		Compound	R ₂	PfPFT % Inhibition at			ED ₅₀ (nM)	
		50 nM	5 nM	0.5 nM	3D7	K1			50 nM	5 nM	0.5 nM	3D7	K1
35		93	64	18	230	1005	59		94	62		450	2800
36		96	65	17	189	932	60		96	93	17	144	965
37		95	66	18	440	240	61		98	82	19	51	210
38		82	37		1600	2200	62		100	93	42	45	56
39		81	32	4	300	250	63		97	66		140	600
40		91	48	9	230	240	64		98	79	10	370	400
41		86	80	35	130	170	65		100	93	4	51	100
42		97	70	9	133	75	66		95	89		105	490
43		97	80	24	250	375	67		96	94	66	600	900
44		98	78	27	320	270	68		66	15		520	750
45		92	52	6	1250	2600	69		96	84	49	210	405
6		100	89	19	155	180	70		98	87	32	700	700
46		90	47	14	510	400	71		91	50	11	430	2500
47		96	77	28	100	100	72		100	82	19	230	1250
48		95	68	6	18	45	73		91	38	0	650	3000
49		99	84	25	230		74		96	71	9	200	650
50		90	59	15	230	400	75		98	81	22	120	600
51		89	69	26	250	600	76		95	53	1	300	1500
52		65	11	6	2700	>5000	77		97	69		143	617
53		32	7	0	>5000	>5000	78		90	52		850	850
54		18	6	0			79		53	11		450	590
55		99	96	74	17	10							
56		99	96	68	13	20							
57		95	91	67	12	16							
58		84	39		750	690							

Table 1. Continued^a

Compound	R ₂	Pf-PFT % Inhibition at			ED ₅₀ (nM)		Compound	R ₂	Pf-PFT % Inhibition at			ED ₅₀ (nM)	
		50 nM	5 nM	0.5 nM	3D7	K1			50 nM	5 nM	0.5 nM	3D7	K1
80		85	31	12	175	98	85		96	77	46	1875	
81		53	4		3000	3000	86		92	63		820	3600
82		88	41	10	810	1450	87		84	32	0	2150	1425
83		88	46	17	1738	1315	88		90	51	0	350	200
84		55	13		2750		89		97	81	24	1000	800
							90		81	33	6	2100	2600

^a All prepared according to Scheme 1.

THQ compounds with a 6-phenyl instead of 6-CN were available to us from a different drug discovery program. Some of these compounds maintain modest potency as inhibitors of Pf-PFT and as antimalarials (**266**, **267**), but in general, we could not find a 6-phenyl THQ with a potency approaching our best compounds in the 6-CN-THQ series. It may be noted that the length of the phenyl is about the same as the length of the CN group, and thus, compounds like **267** may be binding to Pf-PFT in the same way as the 6-CN-THQ compounds, but we have no experimental evidence for this.

The data in Table 9 shows that replacement of the 6-CN group on the THQ core with various amides or a carboxylate is very detrimental to Pf-PFT binding and parasite killing.

Structural Rational of the Structure–Activity Results for THQ-Based PFT Inhibitors. To date, we have not been able to obtain Pf-PFT in amounts sufficient for crystallization trials. However, the X-ray structure of rat and human PFTs are available alone and with a number of bound inhibitors, including the structure of the rat-PFT/**162** complex.⁸ As described in General Methods, we made a homology model of Pf-PFT based on this experimental structure. Most of the residues in the **162** binding site are conserved between rat- and Pf-PFT. The only differences are that Pro-150 β of rat-PFT, which resides in the vicinity of the terminal methyl of the R₂ carbamate of **162**, is replaced with Thr-512 β in Pf-PFT. Tyr-93 β , adjacent to the 6-CN of **162**, is Leu-443 β in Pf-PFT. Two more conservative changes, somewhat further away from **162**, play a role in the binding of other THQ-based inhibitors discussed in this paper: Tyr-166 α (Phe-151 α in Pf-PFT) and Phe-360 β (Tyr-836 β in Pf-PFT). Thus, the crystal structure of the complex of **162** with the rat enzyme is of great value despite only 23% sequence identity for rat- versus Pf-PFT α -subunits and 37% identity between the β -subunits.

The elucidation of the structure–activity relationships of **162** and other THQ-based PFT inhibitors is complicated by the use of racemates. Each compound is a mixture of two enantiomers due to the chiral center at carbon-3 of the THQ ring (Figure 1).

Moreover, each enantiomer can exist in two conformations, with the 3-substituent either axial or equatorial. Hence, it is crucial to know which of the two enantiomers block the enzyme. To gain insight, we first determined the IC₅₀ of the individual enantiomers of **162**. This was carried out by coupling 6-cyano-1,2,3,4-tetrahydro-quinolin-3-ylamine hydrochloride to *S*-mandelic acid and separating the diastereomers as described.^{5,10} The two enantiomeric amines were then converted to the two enantiomers of **162**, **163**, and **164**, as shown in Scheme 1. The *R*-enantiomer of **162**, **163**, displayed an IC₅₀ against Pf-PFT that is 10 times below that of the *S*-enantiomer, **164** (Table 3). This difference is recapitulated in the observed ED₅₀s for blocking *P. falciparum* growth. The 10-fold difference in enzyme binding is modest, corresponding to a difference in binding energy of 1.3 kcal/mol. Superposition of the two enantiomers shows that the first substituent atoms of the two possible equatorial enantiomers at C3 of the THQ ring are only 0.8 Å apart, thereby, allowing for the C3 substituents to adopt similar positions in the binding site regardless of the stereochemistry (Figure 2).

Figure 3 (top panels) shows the experimental, ternary structure of rat-PFT with bound **162** inhibitor and farnesyl-pyrophosphate substrate.⁸ The THQ ring of **162** stacks face-on-face and at an angle of about 25° with Tyr 361 β (Tyr 837 β in the Pf-PFT homology model), projecting the *N*-methyl-imidazole so that it coordinates the catalytic Zn²⁺ of the enzyme (Figure 3). The 6-CN sits in a narrow groove made by Leu-96 β (Leu 446 β in Pf-PFT), Trp-106 β (Trp-456 β in Pf-PFT), Asp-359 β (Asp-835 β in Pf-PFT), and Tyr-361 β (Tyr-837 β in Pf-PFT). In this way, the 6-CN-benzo group of **162** adopts a similar but not identical position as the group of 3-benzyl-1-(3*H*-imidazol-4-ylmethyl)-4-(thiophene-2-sulfonyl)-2,3,4,5-tetrahydro-1*H*-benzo[*e*][1,4]-diazepine-7-carbonitrile (BMS-214662), a tetrahydrobenzodiazepine-based PFT inhibitor for which an X-ray structure of its complex with rat PFT has been published;¹¹ the difference in 6-CN-benzo group atoms ranges from 0.5 to 0.9 Å (Figure 3, bottom left panel). The X-ray structure of bound **162** (obtained

Table 2. Continued^a

Compound	R ₂	Pf-PFT % Inhibition at			IC ₅₀ (nM)	ED ₅₀ (nM)		Compound	R ₂	Pf-PFT % Inhibition at			IC ₅₀ (nM)	ED ₅₀ (nM)	
		50 nM	5 nM	0.5 nM		3D7	K1			50 nM	5 nM	0.5 nM		3D7	K1
138		99	94	18	60	230	143		99	96	57	140	100		
139		99	91	37	210	600	144		99	91	12	355	350		
140		92	20	0	490	890	145		99	90	30	390			
141		98	97		14	18	146		99	99	66	20	<20		
142		97	96	90	40	130									

^a All prepared according to Scheme 1 except compound **104** (Scheme 2).

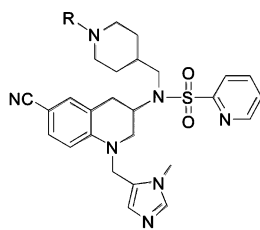
by soaking the rat PFT crystals with racemic **162**) shows that only one enantiomer binds; the data is consistent with our observation that the enantiomer **163** is the better inhibitor (see above). The C3 substituent is equatorial, reflecting the 2.7 kcal/mol calculated preference for this conformation over the axial one in solution. The 2-pyridyl R₁ substituent makes a hydrogen bond with Tyr-361 β (Tyr-837 β in Pf-PFT) and stacks against the second isoprene unit of farnesyl-pyrophosphate. The 2-pyridyl also stacks against the Zn²⁺-binding *N*-Me-imidazole of **162**. The R₂ substituent resides in a large, mainly hydrophobic pocket, which is normally occupied by the side chain of the X residue of the CaaX motif of proteins that are farnesylated (Figure 3, bottom right panel). The R₂ group only partially fills this pocket. The carbonyl oxygen of the carbamate portion of the R₂ substituent of **162** accepts hydrogen bonds with the side chains of Ser-99 β and Trp-102 β of rat-PFT (Ser-449 β and Trp-452 β in Pf-PFT). The terminal Me of the carbamate portion of the R₂ group makes hydrophobic contacts with the side chains of His-149 β (His-509 β in *P. fal.*) and Ala-151 β (Ala-511 β in Pf-PFT). The R₂ piperidine contacts Trp-102 β (Trp-452 β in Pf-PFT). Remarkably, the two oxygens of the sulfonamide do not make direct hydrogen bonds to the protein.

We used the **162**/PFT structural information as a starting point for constructing models of many of the other THQ-based PFT inhibitors prepared in this paper. Rather than discuss each compound, we describe the trends that are supported by the structural information. Figure 4 (top panel) shows the predicted binding mode of **162** in the active site of Pf-PFT. As already noted, THQ-based compounds in Table 1 have a 6-CN group, R₁ = 2-pyridyl, and variation of the R₂ group. Most of the compounds in Table 1 are predicted to be able to bind with R₂ in the a₂X region of the Ca₂a₂X pocket, while maintaining the pose of the THQ scaffold and R₁ and R₃ groups as seen experimentally. R₂ groups that end in a polar group are poor Pf-PFT binders because they cannot interact favorably with the largely hydrophobic environment (**38**, **39**, **52**, **53**, **54**, **90**). Moreover, THQs with small R₂ groups (**38**, **52**, **53**, **90**) barely fill the pocket and therefore display poor enzyme inhibition. On the other hand, the R₂ group of **87** is too large to fill the pocket. Long, linear R₂ groups, some with a small branch, that provide several apolar atoms work better as Pf-PFT inhibitors as they can reach Trp-456 β , Trp-452 β , Ala-511 β , and His-509 β , but this comes at a cost of the loss in conformational entropy when the flexible side chain rigidifies in the active site of Pf-PFT (**35**, **36**, **40**, **41**, **42**, **43**, **44**, **45**, **48**, **46**, **47**, **49**, **50**, **38**).

The R₂ groups of all other THQs contain one or more rings. The best R₂ groups have a short ethylene linker (thus minimizing entropic cost of enzyme binding) followed by a five-membered, aromatic heterocycle (**55**, **56**, **57**). They are predicted to bind in the same way as **162** (Figure 4, top right), engaging in extensive hydrophobic interactions with Leu-446 β , Trp-456 β , Trp-452 β , and C4 of their own THQ scaffold; the latter probably stabilizes the enzyme-bound R₂ conformation for the inhibitor free in solution. Two of the R₂ ring atoms remain solvent exposed, which explains why those two positions can be replaced by nitrogen atoms (**56**, **57**). However, a slightly larger benzene ring cannot be accommodated in the same position (**74**, **75**, **76**), but further *para*-substitution with MeSO₂ leads to two hydrogen bonds of this group with Arg-564 β and Gln-152 α , plus hydrophobic contacts with His-509 β (**69**), explaining the decent potency of this compound. Expansion of the pyrrole ring to an indole (**64**) leads to reduced inhibition because the R₂ conformation cannot be maintained due to steric clash with Leu-446 β . Expansion of the pyrrole ring to phthalimide (**85**) also leads to a different conformation because of steric reasons, though the benzo part is now predicted to interact with His-509 β .

Most R₂ groups with a single methylene linker to an aromatic ring are unable to make an efficient contact with the hydrophobic residues in the pocket of Pf-PFT as the ethylene-linked ones, even when they in turn carry a hydrophobic substituent (**58**, **59**, **60**, **61**, **62**, **63**, **65**, **66**, **68**, **70**, **71**, **69**, **73**, **77**, **78**, **79**, **80**, **81**, **83**, **6**, **84**). Longer linkers to a ring also do not allow for efficient contact of hydrophobic residues in the pocket (**82**, **86**, **88**).

Replacement of the sulfonamide group of THQs with amides universally leads to a loss of binding to Pf-PFT (Table 6). In the crystal structure of rat PFT with **162**, and by homology with Pf-PFT, the sulfonamide moiety adopts a known low-energy conformation. Sulfonamides, which have a pyramidalized nitrogen atom, adopt two low-energy conformations because the N-S bond has partial double character. One is eclipsed, thereby allowing for maximal overlap of the nitrogen lone pair electrons and the S=O bonds (Figure 5). The other one is obtained by nitrogen inversion, thereby reducing the steric interactions.¹² Ab initio calculations at the MP2/6-31+G* level for the model compound *N,N*-dimethylmethanesulfonamide, the closest analog to the sulfonamide substructure in our molecules, shows that this compound prefers the inverted conformation with a C-N-S=O torsion angle of 30°.¹³ This conformation is similar to what is observed in the X-ray structure of **162** bound

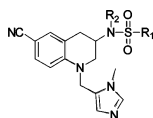
Table 3. Analogs of **6** with a Variation of the R Group Attached to the Piperidine N

Compound	Syn. Scheme	R	Pf-PFT				ED ₅₀		Compound	Syn. Scheme	R	Pf-PFT				ED ₅₀	
			% Inhibition at 50 nM	% Inhibition at 5 nM	IC ₅₀ (nM)	3D7	K1	% Inhibition at 50 nM				% Inhibition at 5 nM	IC ₅₀ (nM)	3D7	K1		
147	2		94	65	29	2.4	37	95	164	1		98	70	02	2.7	95	75
148	2		99	82	20	0.8	16	25	Isomer(S)								
149	2		98	91	24	0.6	18	13	165	2		100	95	46	0.5	55	40
150	2		99	76	17	1.2	48	75	166	2		97	90	36		50	50
151	2		96	88	36	0.6	20	76	167	2		100	88	12	1.4	62	62
152	2		95	63	12	3	80	690	168	2		91	91	47		65	75
153	2		100	94	39	0.75	11.5	10	169	2		98	66	13		550	650
154	2		100	94	39		58	50	170	2		98	95	60	0.65	67	65
155	2		98	77	30	2	43	55	171	2		100	94	35		13	11.5
156	2		100	92	31		50	60	172	2		100	93	38		65	45
157	2		88	37	15		750	690	173	2		98	84	28		320	150
158	2		94	63	20	7	150	330	174	2		99	91	31		35	65
159	2		26	7	0	900	460	1700	175	2		94	62	14		140	200
160	2		92	92	51		80	93	176	2		38	0	0		3000	2800
161	2		99	87	35		70	81	177	2		99	93	45	0.9	62	50
162	2		100	96	61	0.58	16	15	178	2		98	94	56		75	55
163	1								179	2		96	89	17		75	55
Isomer (R)	1		100	99	58	0.29	11	13	180	2		96	67	7		275	280
									181	2		92	60	20		700	650

to rat PFT (Figure 5). Simple stereochemical considerations indicate why the amide analogs of our sulfonamide THQ PFTIs are poor inhibitors. The amide function has two trigonal centers, and thus, a planar arrangement of all substituents. This leads to an orientation of the R₁ group in the amides that is 90° off from

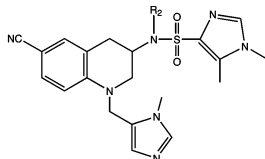
the orientation of the R₁ of **162** (Figure 5), and this altered orientation is sterically disallowed by the active site of the PFT.

Modeling showed that there is space in the active site of Pf-PFT to accommodate groups other than *N*-methyl on the Zn²⁺-binding imidazole. A benzyl (**254**, Table 7) was not very

Table 4. 6-CN-THQs with a Variation of R₁^a

Compound	R ₁	R ₂	P _f -PFT % Inhibition at			IC ₅₀ (nM)	ED ₅₀ (nM)		Compound	R ₁	R ₂	P _f -PFT % Inhibition at			IC ₅₀ (nM)	ED ₅₀ (nM)	
			50 nM	5 nM	0.5 nM		3D7	K1				50 nM	5 nM	0.5 nM		3D7	K1
182			98	93	43	50	70	207			15	0	0	>5000	>5000		
183			99	93	48	100		208			51	7	0	600	>5000		
184			98	79	14	170	190	209			61	11	0	820	2100		
185			65	6	0	1800	2000	210			41	16	11	1200	3050		
186			97	80	24	55	70	211			62	10	8	360	3600		
187			93	86	39	90	150	212			96	76	12	580	500		
188			98	84	20	140	160	213			94	62	23	175	175		
189			88	39	2	550	1700	214			86	44	10	730	750		
190			95	80	24	260	400	215			66	22	13	900	1000		
191			99	99	72	3	1.6	216			25	4	4	150	150		
192			96	67	15	38		217			74	28	4	700	1000		
193			100	96	39	60	75	218			99	91	38	165	330		
194			95	66	18	55	75	219			97	83	17	185	340		
195			99	86	25	62	140	220			99	87	16	400	800		
196			92	61	10	2300	1900	221			100	100	84	<20	<20		
197			89	49	5	>5000	675	222			97	88	36	75	60		
198			100	98	39	42	45	223			97	78	10	2100	3500		
199			66	5	0	2700	>5000	224			97	55	13	830			
200			44	00	0	4100	>5000	225			96	67	8	600			
201			55	22	1	1100	1800	226			80	27	2	8	750	3100	
202			37	3	0	>5000	3950	227			15	14	10	800	>5000	>5000	
203			58	19	0	1600	2400	228			3	0	0	>5000	>5000		
204			99	81	24	138	105	229			0	3	2	>5000	>5000		
205			99	89	31	135	100	230			11	2	5	>5000	>5000		
206			68	21	2	>5000	>5000	231			11	10	5	>5000	>5000		
								232			60	21	14	>5000	>5000		
								233			71	33	30	42	>5000	5000	

^a All prepared according to Scheme 1.

Table 5. 6-CN-THQs with Dimethyl Imidazole^a


Comp.	R ₂	Pf-PFT % Inhibition at			ED ₅₀ (nM)	
		50 nM	5 nM	0.5 nM	3D7	K1
234		100	97	49	35	<20
235		98	87	18	140	75
236		92	70	23	320	450
237		97	76	10	640	
238		98	87	13	850	

^a All were prepared according to Scheme 1.

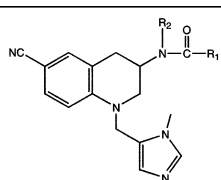
effective probably because of the extra entropy loss due to two extra rotatable bonds. Replacement of the methylene linker in the Zn²⁺-binding arm (attached to N1 of the THQ ring) by an SO₂ (**255**, Table 7) leads to an inactive compound. This is most likely because of the increased electron-withdrawing character of the SO₂ linker, thereby decreasing the basicity of the imidazole N and, thus, the coordination affinity to the active site Zn²⁺. Using the SPARC v3.1 program,^{14,15} we calculated that the pK_a of the protonated imidazole drops from 6.8 to 5.1 when the CH₂ linker is replaced with SO₂. If the drop in proton affinity is the same for Zn²⁺, this drop in pK_a of 1.7 would give a drop in IC₅₀ by 50-fold.

Replacement of the 6-CN group with phenyl is tolerated (Table 8). Replacement with more polar substituents (Table 9) is not tolerated, which is consistent with the lack of appropriate hydrogen bond donors and acceptors in the pocket on Pf-PFT that binds the 6-CN group.

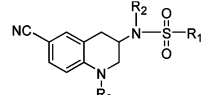
Inhibition of Mammalian PFT. A subset of THQ-based PFTIs were tested for inhibition of rat PFT, and results are summarized in Table 10 and compared to those obtained with Pf-PFT. Most compounds displayed comparable potency on both enzymes. The exceptions are **84** and **129**, which are about 10-fold more potent on Pf-PFT than on rat PFT, and **126**, which shows the reverse preference. As noted in our earlier publications, clinical trials have shown that PFTIs are well tolerated in man after several weeks of continuous dosing. Thus, specificity toward Pf-PFT versus mammalian PFT is probably not required for a drug that would be used to treat malaria over the course of a few days.

Conclusions

In this study we show that THQ-based PFTIs are potent inhibitors of Pf-PFT activity and of erythrocytic stage *P. falciparum* growth. Several compounds were found with growth inhibition potency down in the low nanomolar range, with several compounds blocking parasite growth at concentrations

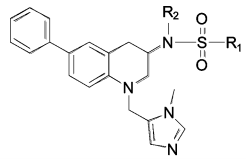
Table 6. 6-CN-THQs with Amides^a


Compound	R ₁	R ₂	Pf-PFT % Inhibition at			IC ₅₀ (nM)	ED ₅₀ (nM)	
			50 nM	5 nM	0.5 nM		3D7	K1
239						>50	>5000	>5000
240						>50	>5000	>5000
241						>50	>5000	>5000
242			26	9	6		2900	
243			56	19	11		290	
244			33	0	0		690	750
245			43	1	0		650	730
246			33	0	0		950	2000
247			52	9	0		270	450
248			16	0	0		2700	
249			92	51	0		260	
250			66	13	0		340	
251			88	39	0		75	

^a All were prepared according to Scheme 3.**Table 7.** 6-CN-THQs with a Variation of R₃


Comp	Syn Scheme	R ₁	R ₂	R ₃	Pf-PFT % Inhibition at			ED ₅₀ (nM)	
					50 nM	5 nM	0.5 nM	3D7	K1
252	4				94			120	
253	4				93			120	
254	4				45	22	150	140	
255	5				0	0	0	>5000	3200
34	8				96	79	12	650	650
256	4				35	12	3	3400	3000

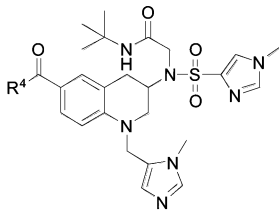
<5 nM. A good deal of the structure–activity data for the inhibition of Pf-PFT can be accounted for based on the structural consideration of one of the compounds, **162**, bound to mammalian PFT. In a companion study, we have carried out detailed

Table 8. 6-Phenyl-THQs^a


Compound	R ₁	R ₂	Pf-PFT % Inhibition at			ED ₅₀ (nM)	
			50 nM	5 nM	0.5 nM	3D7	K1
257		H	80	31	14	3500	>5000
258			88	38	10	>5000	>5000
259			86	29	10	5000	>5000
260			98	84	27	3000	3700
261			95	74	14	>5000	3700
262			98	84	34	1500	
263			99	89	22	640	475
264			97	89	21	380	360
265			97	91	28	750	950
266			99	87	37	375	350
267			97	73	23	381	395
268			99	91	29	400	700
269			98	81	18	2400	750
270			32	0	0	450	350
271			33	10	0	860	
272			90	38	0	460	150
273			88	46	0	4600	3500
274			79	26	0	3000	3700
275			99	90	9	450	380
276			46	0	0	2900	1800
277			98	81	12	300	500
278			98	84	32	270	450
279		H	19	14	11	>5000	>5000
280			11	6	6	>5000	3000
281			22	15	0	2700	
282			2	0	0	>5000	>5000
283			10	1	4	3500	>5000
284			8	0	0	2800	2800

^a All were prepared according to Scheme 6.

preclinical pharmacokinetic studies of our most potent Pf-PFT inhibitors.⁹ Together, these two studies provide the basis for further development of Pf-PFT inhibitors as novel antimalarial drugs.

Table 9. 6-Acyl-THQs^a


Compound	R ₄	Pf-PFT % Inhibition at			ED ₅₀ (nM)	
		50 nM	5 nM	0.5 nM	3D7	K1
285		25	0	4	>5000	>5000
286		46	7	14	4000	2600
287		66	17	5	2800	2300
288		35	2	0	>5000	
289		80	29	0	3500	1425
290		69	20	12	1200	ND
291		59	1	0	4600	ND
292		73	23	0	2800	2600

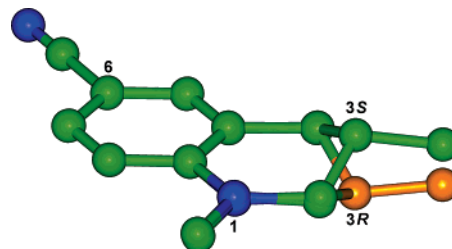
^a All were prepared according to Scheme 7.

Figure 2. Near coincidence of the sulfonamide nitrogen positions of the C3 enantiomers of THQ inhibitors like **162**. The figure shows the superposition of the two possible envelope conformations of the THQ ring, resulting in the positions of the exocyclic sulfonamide nitrogens being only 0.8 Å apart (only the equatorial conformations are shown; they are 2.7 kcal/mol more stable than the axial conformations). The *R/S* designation is specifically for the sulfonamide substitution. All figures of 3-dimensional molecular scenes were made with PyMOL (<http://www.pymol.org>).

Experimental Section

Synthesis of Compounds. General Methods. Unless otherwise indicated, all anhydrous solvents were commercially obtained and stored under nitrogen. Reactions were performed under an atmosphere of dry nitrogen in oven-dried glassware and were monitored for completeness by thin layer chromatography (TLC) using silica gel 60 F-254 (0.25 mm) plates with detection with UV light. ¹H NMR spectra were recorded on dilute solutions in CDCl₃, CD₃-OD, or DMSO-*d*₆ at 300 or 500 MHz. Chemical shifts are reported in parts per million (δ) downfield from tetramethylsilane (TMS). Coupling constants (*J*) are reported in Hz. Electrospray ionization mass spectra were acquired on an Bruker Esquire LC00066. Flash chromatography was carried out with silica gel (40–63 μm). Preparative reverse phase HPLC was performed on an automated

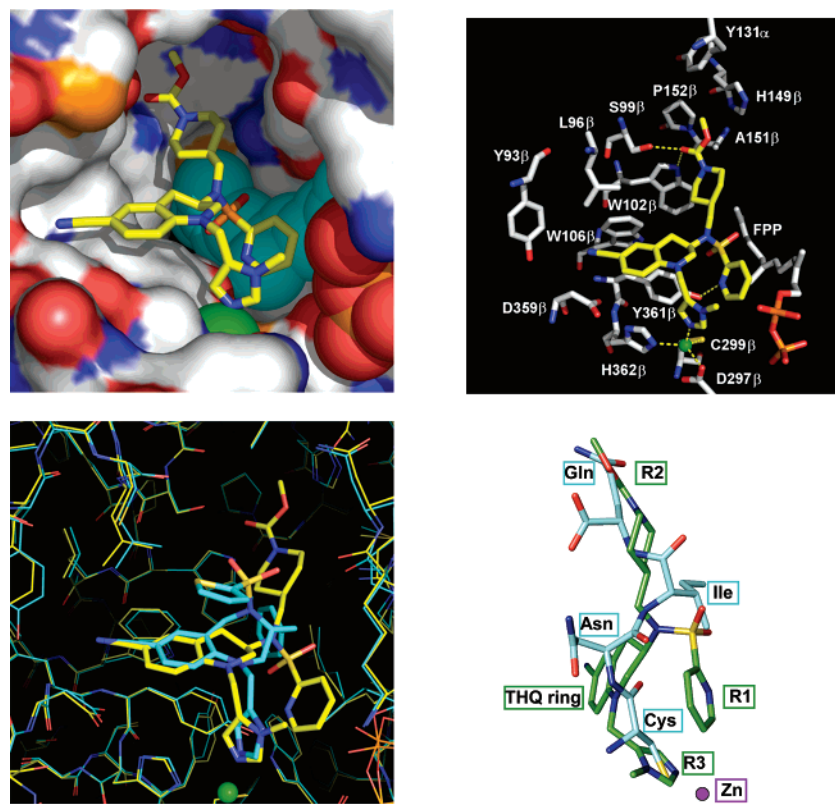


Figure 3. Experimental binding mode of **162** to rat PFT (top left); molecular surface of rat-PFT (left; C, gray; N, blue; O, red; S, orange), with farnesyl-pyrophosphate (red, orange, and cyan) and Zn^{2+} (green) in CPK representation and **162** in stick model representation; equivalent all-stick model (top right); comparison of the binding modes of **162** (yellow carbons) and 3-benzyl-1-(3*H*-imidazol-4-ylmethyl)-4-(thiophene-2-sulfonyl)-2,3,4,5-tetrahydro-1*H*-benzo[*e*][1,4]diazepine-7-carbonitrile (cyan carbons, see ref 11 for the structure) to rat PFT (bottom left); superposition of **162** (green carbon atoms) and the C-terminal tetrapeptide fragment of the Rap2a peptide farnesyl acceptor substrate (cyan carbon atoms) as bound in PFT (bottom right; catalytic Zn^{2+} shown).

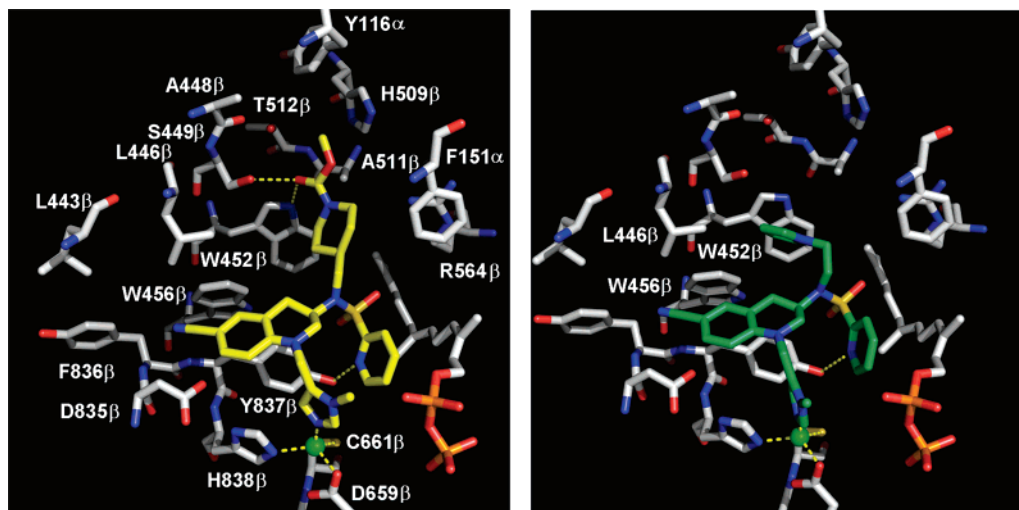


Figure 4. Predicted binding mode of **162** in the active site of Pf-PFT (top left); molecular surface of PFT (left; C, gray; N, blue; O, red; S, orange), with farnesyl-pyrophosphate (red, orange, and cyan) and Zn^{2+} (green); predicted binding mode of **55** in the active site of Pf-PFT (top right). Note how the R_2 pyrrole group is wedged between C4 of the THQ ring and Trp-452 β and Trp-456 β .

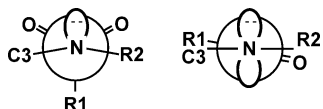


Figure 5. Comparison of the experimentally observed conformation of THQ PFTIs with a sulfonamide linker (left) and the conformation accessible to the analogous amides (right). The latter projects the R_1 group into a sterically poorly accessible area of PFT (not shown).

Varian Prep star system using a gradient of 20% MeOH to 100% MeOH (with 0.1% trifluoroacetic acid) over 30 min using a YMC S5 ODS column (20 × 100 mm, Waters, Inc.). All final compounds

(those tested on Pf-PFT and on parasites cultures) were purified by HPLC as above to single eluting peaks.

General Procedure for Synthesis of Compounds According to Scheme 1. Sulfonation. A solution of 6-cyano-1,2,3,4-tetrahydroquinolin-3-ylamine hydrochloride **3** (5 mmol), sulfonyl chloride (10 mmol; for example, ref 16, and *N,N*-diisopropylethyl amine (15 mmol) in 25 mL of anhydrous CH_3CN was stirred at room temperature overnight. A light-colored precipitate of **4** was isolated by vacuum filtration. More often, product **4** was obtained by flash chromatography on a silica gel column, eluting with 50% ethyl acetate/hexane: yields 85–95%.

Table 10. Potency on Mammalian versus Pf-PFT

cmpd	IC ₅₀ on mammalian PFT (nM)	Approximate IC ₅₀ on Pf-PFT ^a (nM)
81	10	50
65	3.8	2
84	440	50
55	1.7	0.2
62	3	0.5
6	7	2
226	5	20
151	7.8	2
152	6.5	4
162	3.2	0.4
158	16	4
167	25	3
165	5.5	0.5
134	2.6	0.5
129	1000	40
91	7.5	2
101	105	40
126	4.8	40
123	3.4	1

^a IC₅₀ values were estimated based on the % inhibition of Pf-PFT at 0.5, 5, and 50 nM inhibitor using the data in Tables 1–9.

1-Methyl-1*H*-imidazole-4-sulfonic Acid [6-Cyano-1,2,3,4-tetrahydro-quinolin-3-yl]-amide (4). ¹H NMR (500 MHz, DMSO-*d*₆) δ 7.80 (s, 1H), 7.78 (s, 1H), 7.70 (br s, 1H), 7.25 (d, *J* = 8.7 Hz, 1H), 7.20 (s, 1H), 6.81 (s, 1H), 6.51 (d, *J* = 8.6 Hz, 1H), 3.78 (s, 3H), 3.52–3.43 (m, 1H), 3.25–3.20 (m, 1H), 3.15–2.9 (m, 1H), 2.81–2.73 (m, 1H), 2.65–2.53 (m, 1H). MS *m/z* 318.5 (M + H⁺).

Pyridine-2-sulfonic Acid [6-Cyano-1,2,3,4-tetrahydro-quinolin-3-yl]-amide (4). ¹H NMR (300 MHz, methanol-*d*₄) δ 8.51 (d, *J* = 7.2 Hz, 1H), 8.02 (td, *J* = 2.1, 7.8 Hz, 1H), 7.92 (dt, *J* = 1.8, 7.5 Hz, 1H), 7.47 (ddd, *J* = 1.2, 4.8, 7.5 Hz, 1H), 7.12 (dd, *J* = 2.1, 8.4 Hz, 1H), 7.0 (d, *J* = 1.8 Hz, 1H), 6.3 (d, *J* = 8.4 Hz, 1H), 5.87 (d, *J* = 7.8 Hz, 1H), 3.94–4.01 (m, 1H), 3.36 (dd, *J* = 2.7, 12 Hz, 1H), 3.25 (ddd, *J* = 2.1, 4.5, 12.3 Hz, 1H), 2.87 (dd *J* = 4.2, 16.5 Hz, 1H), 2.71 (ddd, *J* = 2.1, 4.8, 16.5 Hz, 1H). MS *m/z* 315 (M + H⁺).

Reductive Amination. A mixture of sulfonamide **4** (5 mmol), 1-methyl-1*H*-imidazole-5-carboxaldehyde (10 mmol),¹⁶ and 20 mL of 50% trifluoroacetic acid in dichloroethane was warmed at 50 °C under argon. After 2 h, triethylsilane (20 mmol) was added. After 48 h, the solvent was removed under reduced pressure, and the crude product was partitioned between methylene chloride and 1 N NaOH (45 mL). The organic layer was separated, and the aqueous layer was extracted with CH₂Cl₂ (3 × 25 mL). The combined organic layers were dried over MgSO₄, filtered, and concentrated. The crude residue was either recrystallized with dichloromethane or purified on a flash silica gel chromatography to afforded **5** in 45–50% yield.

1-Methyl-1*H*-imidazole-4-sulfonic Acid [6-Cyano-1-(3-methyl-3*H*-imidazol-4-ylmethyl)-1,2,3,4-tetrahydro-quinolin-3-yl]-amide Trifluoro Acetate Salt (5). Recrystallized from CH₂Cl₂ afforded the product as a white solid (70%). ¹H NMR (300 MHz, methanol-*d*₄) δ 8.89 (s, 1H), 7.82 (s, 1H), 7.72 (s, 1H), 7.41 (s, 1H), 7.36 (d, *J* = 8.2 Hz, 1H), 7.22 (s, 1H), 6.80 (d, *J* = 8.6 Hz, 1H), 4.80 (d, *J* = 16.80 Hz, 1H), 4.65 (d, *J* = 16.80 Hz, 1H), 3.87 (s, 3H), 3.85–3.79 (m, 1H), 3.78 (s, 3H), 3.55 (dd, *J* = 11.9 Hz, 1H), 3.42 (dd, *J* = 12.4 Hz, 1H), 3.05 (dd, *J* = 15.78 Hz, 1H), 2.71 (dd, *J* = 15.78 Hz, 1H). MS *m/z* 412.5 (M + H⁺).

Pyridine-2-sulfonic Acid [6-Cyano-1-(3-methyl-3*H*-imidazol-4-ylmethyl)-1,2,3,4-tetrahydro-quinolin-3-yl]-amide (5). ¹H NMR (300 MHz, DMSO-*d*₆) δ 8.70 (d, *J* = 4.8 Hz, 1H), 8.14 (d, *J* = 6.6 Hz, 1H), 8.06 (dt, *J* = 1.8, 7.5 Hz, 1H), 7.99 (s, 1H), 7.67 (ddd, *J* = 1.2, 4.8, 7.8 Hz, 1H), 7.37 (dd, *J* = 2.1, 8.7 Hz, 1H), 7.27 (d, *J* = 1.8 Hz, 1H), 6.88 (s, 1H), 6.8 (d, *J* = 8.7 Hz, 1H), 4.62 (d, *J* = 16.5 Hz, 1H), 4.59 (d, *J* = 16.5 Hz, 1H), 3.73–3.85 (m, 1H), 3.60 (s, 3H), 3.38 (dd, *J* = 2.4, 11.7 Hz, 1H), 3.17 (dd, *J* = 8.7, 12.9

Hz, 1H), 2.88 (dd, *J* = 4.2, 15.9 Hz, 1H), 2.70 (dd, *J* = 8.7, 15.9 Hz, 1H). MS *m/z* 409.3 (M + H⁺).

***N*-[6-Cyano-1-(3-methyl-3*H*-imidazol-4-ylmethyl)-1,2,3,4-tetrahydro-quinolin-3-yl]-4-fluoro-benzenesulfonamide (5).** ¹H NMR (500 MHz, methanol-*d*₄) δ 8.35 (s, 1H), 7.95–7.93 (m, 2H), 7.46 (s, 1H), 7.39 (d, *J* = 8.5 Hz, 1H), 7.35 (t, *J* = 8.0 Hz, 2H), 7.24 (s, 1H), 6.82 (d, *J* = 8.5 Hz, 1H), 4.82 (d, *J* = 17.0 Hz, 1H), 4.65 (d, *J* = 17.0 Hz, 1H), 3.95–3.85 (m, 4H), 3.69–3.65 (m, 1H), 3.55–3.45 (m, 1H), 2.97–2.96 (m, 1H), 2.71–2.61 (m, 1H). MS *m/z* 426.12 (M + H⁺).

***N*-Alkylation.** To a suspension of **5** (5 mmol) and Cs₂CO₃ (9.8 mmol) in dry DMF (5 mL) was added the appropriate alkyl halide (5.4 mmol), and the mixture was stirred at room temperature overnight under argon. After addition of water (20 mL), the solution was extracted with ethyl acetate (3 × 20 mL). The organic layer was extracted with brine (3 × 10 mL). The combined organic layers were dried over MgSO₄ and evaporated under reduced pressure. The residue was purified by HPLC.

Pyridine-2-sulfonic Acid [6-Cyano-1-(3-methyl-3*H*-imidazol-4-ylmethyl)-1,2,3,4-tetrahydro-quinolin-3-yl]-[4-methanesulfonyl-benzyl]-amide (69). ¹H NMR (300 MHz, methanol-*d*₄) δ 8.86 (s, 1H), 8.71 (d, *J* = 7.2 Hz, 1H), 8.10 (td, *J* = 1.5, 8.1 Hz, 1H), 7.99 (dt, *J* = 1.2, 8.1 Hz, 1H), 7.90 (d, *J* = 8.1 Hz, 2H), 7.69 (ddd, *J* = 1.2, 4.8, 7.5 Hz, 1H), 7.61 (d, *J* = 8.1 Hz, 2H), 7.33 (dd, *J* = 2.1, 9.0 Hz, 1H), 7.28 (s, 1H), 7.25 (d, *J* = 2.1 Hz, 1H), 6.65 (d, *J* = 8.7 Hz, 1H), 4.79 (d, *J* = 17.1 Hz, 1H), 4.62 (d, *J* = 17.1 Hz, 1H), 4.39–4.59 (m, 3H), 3.8 (s, 3H), 3.55–3.62 (m, 1H), 3.42–3.47 (m, 1H), 3.15 (s, 3H), 3.07–3.14 (m, 1H), 2.97 (dd, *J* = 4.5, 15.9 Hz, 1H). MS *m/z* 577.4 (M + H⁺).

6-[[[6-Cyano-1-(3-methyl-3*H*-imidazol-4-ylmethyl)-1,2,3,4-tetrahydro-quinolin-3-yl]-[pyridine-2-sulfonyl-amino]-methyl]-pyridine-2-carboxylic Acid Methyl Ester (67). ¹H NMR (300 MHz, CDCl₃) δ 8.78 (s, 1H), 8.63 (d, *J* = 7.0 Hz, 1H), 7.78–8.04 (m, 5H), 7.51–7.76 (m, 1H), 7.30–7.34 (m, 2H), 7.18 (s, 1H), 6.56 (d, *J* = 8.7 Hz, 1H), 4.76 (d, *J* = 17.1 Hz, 1H), 4.65 (d, *J* = 17.1 Hz, 1H), 4.47–4.61 (m, 3H), 3.96 (s, 3H), 3.85 (s, 3H), 3.54–3.62 (m, 1H), 3.42–3.51 (m, 1H), 3.13 (dd, *J* = 11.1, 15 Hz, 1H), 2.91 (dd, *J* = 3.6, 15 Hz, 1H). MS *m/z* 558.3 (M + H⁺).

4-[[[6-Cyano-1-(3-methyl-3*H*-imidazol-4-ylmethyl)-1,2,3,4-tetrahydro-quinolin-3-yl]-[pyridine-2-sulfonyl-amino]-methyl]-piperidine-1-carboxylic Acid *tert*-Butyl Ester (6). ¹H NMR (300 MHz, methanol-*d*₄) δ 8.93 (s, 1H), 8.71 (d, *J* = 7.2 Hz, 1H), 8.05 (td, *J* = 1.8, 7.5 Hz, 1H), 8.01–8.02 (m, 1H), 7.66 (ddd, *J* = 1.2, 4.8, 7.5 Hz, 1H), 7.43 (s, 1H), 7.39 (dd, *J* = 1.5, 8.4 Hz, 1H), 7.33 (s, 1H), 6.80 (d, *J* = 9.7 Hz, 1H), 4.81 (d, *J* = 16.8 Hz, 1H), 4.68 (d, *J* = 16.8 Hz, 1H), 4.32–4.44 (m, 1H), 4.05–4.09 (m, 2H), 3.91 (s, 3H), 3.58–3.66 (m, 2H), 3.53–3.55 (m, 1H), 3.11–3.21 (m, 3H), 2.87–2.88 (m, 1H), 2.63–2.69 (m, 1H), 1.64–1.77 (m, 3H), 1.3 (s, 9H), 1.01–1.11 (m, 2H). MS *m/z* 606.6 (M + H⁺).

Pyridine-2-sulfonic Acid [6-Cyano-1-(3-methyl-3*H*-imidazol-4-ylmethyl)-1,2,3,4-tetrahydro-quinolin-3-yl]-[2-pyrazol-1-yl-ethyl]-amide (56). ¹H NMR (300 MHz, methanol-*d*₄) δ 8.92 (s, 1H), 8.73 (d, *J* = 6.9 Hz, 1H), 8.01–8.12 (m, 2H), 7.64–7.71 (m, 1H), 7.61 (d, *J* = 2.1 Hz, 1H), 7.50 (d, *J* = 1.5 Hz, 1H), 7.32–7.38 (m, 2H), 7.21 (s, 1H), 6.79 (d, *J* = 8.7 Hz, 1H), 6.30 (t, *J* = 2.1 Hz, 1H), 4.68 (d, *J* = 18.3 Hz, 1H), 4.60 (d, *J* = 18.3 Hz, 1H), 4.70 (t, *J* = 6.3 Hz, 2H), 4.25–4.35 (m, 1H), 3.83 (s, 3H), 3.74 (t, *J* = 6.3 Hz, 2H), 3.10–3.21 (m, 2H), 2.86 (dd, *J* = 12, 15.3 Hz, 1H), 2.58 (dd, *J* = 3.9, 15.3 Hz, 1H). MS *m/z* 503.4 (M + H⁺).

3-[[[6-Cyano-1-(3-methyl-3*H*-imidazol-4-ylmethyl)-1,2,3,4-tetrahydro-quinolin-3-yl]-[pyridine-2-sulfonyl-amino]-propyl]-methyl-carbamic Acid Methyl Ester (48). ¹H NMR (300 MHz, methanol-*d*₄) δ 8.94 (d, *J* = 0.9 Hz, 1H), 8.70 (d, *J* = 7.5 Hz, 1H), 8.08 (td, *J* = 1.8, 7.8 Hz, 1H), 8.0 (dt, *J* = 1.2, 7.8 Hz, 1H), 7.66 (ddd, *J* = 1.5, 4.8, 7.5 Hz, 1H), 7.43 (d, *J* = 1.2 Hz, 1H), 7.38 (dd, *J* = 2.1, 8.7 Hz, 1H), 7.33 (s, 1H), 6.81 (d, *J* = 8.7 Hz, 1H), 4.82 (d, *J* = 17.5 Hz, 1H), 4.62 (d, *J* = 17.5 Hz, 1H), 4.40–4.52 (m, 1H), 3.92 (s, 3H), 3.65 (s, 3H), 3.55–3.47 (m, 4H), 3.28–3.05 (m, 4H), 2.93 (s, 3H), 1.78–1.88 (m, 2H). MS *m/z* 538.4 (M + H⁺).

Pyridine-2-sulfonic Acid [6-Cyano-1-(3-methyl-3*H*-imidazol-4-ylmethyl)-1,2,3,4-tetrahydro-quinolin-3-yl]-(4-fluoro-benzyl)-amide (71). ¹H NMR (300 MHz, methanol-*d*₄) δ 8.89 (s, 1H), 8.74 (d, *J* = 6.5 Hz, 1H), 8.09 (td, *J* = 1.8, 7.8 Hz, 1H), 8.0 (dt, *J* = 1.2, 7.8 Hz, 1H), 7.67 (ddd, *J* = 1.5, 4.8, 7.5 Hz, 1H), 7.39–7.43 (m, 2H), 7.35 (dd, *J* = 2.1, 8.7 Hz, 1H), 7.33 (s, 1H), 7.25 (s, 1H), 7.01–7.07 (m, 2H), 6.75 (d, *J* = 8.7 Hz, 1H), 4.43–4.69 (m, 5H), 3.82 (s, 3H), 3.55–3.47 (m, 1H), 3.17–3.25 (m, 1H), 3.07 (dd, *J* = 12, 15 Hz, 1H), 2.91 (dd, *J* = 3.9, 15 Hz, 1H). MS *m/z* 517.4 (M + H⁺).

Pyridine-2-sulfonic Acid [6-Cyano-1-(3-methyl-3*H*-imidazol-4-ylmethyl)-1,2,3,4-tetrahydro-quinolin-3-yl]-[2-(2-trifluoromethyl-phenyl)-ethyl]-amide (76). ¹H NMR (300 MHz, methanol-*d*₄) δ 8.87 (s, 1H), 8.74 (d, *J* = 4.5 Hz, 1H), 8.12 (td, *J* = 1.8, 7.8 Hz, 1H), 8.0 (dt, *J* = 1.2, 7.8 Hz, 1H), 7.63–7.71 (m, 2H), 7.58–7.63 (m, 1H), 7.37–7.49 (m, 5H), 6.81 (d, *J* = 8.7 Hz, 1H), 4.92 (d, *J* = 17.7 Hz, 1H), 4.82 (d, *J* = 17.7 Hz, 1H), 4.50–4.56 (m, 1H), 3.98 (s, 3H), 3.55–3.47 (m, 4H), 3.18–3.31 (m, 3H), 3.02–3.08 (m, 1H). MS *m/z* 581.4 (M + H⁺).

1-Methyl-1*H*-imidazole-4-sulfonic Acid [6-Cyano-1-(3-methyl-3*H*-imidazol-4-ylmethyl)-1,2,3,4-tetrahydro-quinolin-3-yl]-[2-(2-fluoro-phenyl)-ethyl]-amide (113). ¹H NMR (300 MHz, methanol-*d*₄) δ 8.93 (s, 1H), 7.76 (s, 1H), 7.73 (s, 1H), 7.51 (s, 1H), 7.38 (dd, *J* = 2.1, 8.7 Hz, 1H), 7.23–7.32 (m, 3H), 7.10–7.17 (m, 2H), 6.84 (d, *J* = 8.6 Hz, 1H), 4.92 (d, *J* = 17.7 Hz, 1H), 4.82 (d, *J* = 17.7 Hz, 1H), 4.48–4.50 (m, 1H), 4.07 (s, 3H), 3.82 (s, 3H), 3.35–3.57 (m, 4H), 3.16–3.29 (m, 3H), 2.92–3.00 (m, 1H). MS *m/z* 534.4 (M + H⁺).

1-Methyl-1*H*-imidazole-4-sulfonic Acid [6-Cyano-1-(3-methyl-3*H*-imidazol-4-ylmethyl)-1,2,3,4-tetrahydro-quinolin-3-yl]-[2-(4-fluoro-phenyl)-ethyl]-amide (112). ¹H NMR (300 MHz, acetone-*d*₆) δ 8.93 (s, 1H), 7.75 (s, 1H), 7.74 (s, 1H), 7.49 (s, 1H), 7.38 (dd, *J* = 2.1, 8.7 Hz, 1H), 7.32 (s, 1H), 7.22–7.25 (m, 2H), 7.01–7.07 (m, 2H), 6.93 (d, *J* = 8.6 Hz, 1H), 4.93 (d, *J* = 16.8 Hz, 1H), 4.80 (d, *J* = 16.8 Hz, 1H), 4.38–4.46 (m, 1H), 4.07 (s, 3H), 3.82 (s, 3H), 3.34–3.54 (m, 4H), 3.07 (dd, *J* = 12, 15 Hz, 1H), 2.98 (t, *J* = 8.1 Hz, 2H), 2.90 (dd, *J* = 3.7, 15.2 Hz, 1H). MS *m/z* 534.4 (M + H⁺).

1-Methyl-1*H*-imidazole-4-sulfonic Acid [6-Cyano-1-(3-methyl-3*H*-imidazol-4-ylmethyl)-1,2,3,4-tetrahydro-quinolin-3-yl]-(4-fluoro-benzyl)-amide (109). ¹H NMR (300 MHz, methanol-*d*₄) δ 8.90 (s, 1H), 7.81 (s, 1H), 7.73 (s, 1H), 7.36–7.42 (m, 3H), 7.33 (s, 1H), 7.27 (s, 1H), 7.10–7.17 (m, 2H), 6.84 (d, *J* = 8.6 Hz, 1H), 4.28–4.65 (m, 5H), 3.87 (s, 3H), 3.80 (s, 3H), 3.34–3.39 (m, 1H), 3.18–3.26 (m, 1H), 3.07 (dd, *J* = 11.4, 15.3 Hz, 1H), 2.87 (dd, *J* = 3.7, 15.2 Hz, 1H). MS *m/z* 520.4 (M + H⁺).

1-Methyl-1*H*-imidazole-4-sulfonic Acid [6-Cyano-1-(3-methyl-3*H*-imidazol-4-ylmethyl)-1,2,3,4-tetrahydro-quinolin-3-yl]-(4-ethanesulfonyl-benzyl)-amide (132). ¹H NMR (300 MHz, methanol-*d*₄) δ 8.87 (s, 1H), 7.87 (d, *J* = 8.1 Hz, 2H), 7.85 (s, 1H), 7.77 (s, 1H), 7.62 (d, *J* = 8.1 Hz, 2H), 7.34 (dd, *J* = 1.8, 8.7 Hz, 1H), 7.25 (d, *J* = 1.8 Hz, 1H), 6.68 (d, *J* = 8.7 Hz), 4.75 (d, 2H), 4.53–4.55 (m, 1H), 4.51 (d, *J* = 17.7 Hz, 1H), 4.45 (d, *J* = 17.7 Hz, 1H), 3.81 (s, 3H), 3.80 (s, 3H), 3.10–3.25 (m, 6H), 2.95–3.05 (m, 1H), 1.21–1.25 (t, 3H). MS *m/z* 594.5 (M + H⁺).

1-Methyl-1*H*-imidazole-4-sulfonic Acid (4-Benzenesulfonyl-benzyl)-[6-cyano-1-(3-methyl-3*H*-imidazol-4-ylmethyl)-1,2,3,4-tetrahydro-quinolin-3-yl]-amide (145). ¹H NMR (300 MHz, methanol-*d*₄) δ 8.89 (s, 1H), 7.89–8.10 (m, 4H), 7.87 (d, *J* = 8.1 Hz, 2H), 7.77 (s, 1H), 7.50–7.72 (m, 5H), 7.34 (dd, *J* = 1.8, 8.7 Hz, 1H), 7.25 (d, *J* = 1.8 Hz, 1H), 6.68 (d, *J* = 8.7 Hz, 1H), 4.75 (m, 2H), 4.53–4.55 (m, 1H), 4.51 (d, *J* = 17.7 Hz, 1H), 4.45 (d, *J* = 17.7 Hz, 1H), 3.81 (s, 3H), 3.80 (s, 3H), 3.40–3.45 (m, 2H), 2.95–3.05 (m, 1H). MS *m/z* 642.6 (M + H⁺).

1-Methyl-1*H*-imidazole-4-sulfonic Acid [6-Cyano-1-(3-methyl-3*H*-imidazol-4-ylmethyl)-1,2,3,4-tetrahydro-quinolin-3-yl]-(4,4-dioxo-3,4-dihydro-2*H*-4*λ*6-benzo[1,4]oxathiin-7-ylmethyl)-amide (146). ¹H NMR (300 MHz, methanol-*d*₄) δ 8.90 (s, 1H), 7.85 (s, 1H), 7.68 (d, *J* = 8.1 Hz, 1H), 7.45 (s, 1H), 7.30 (s, 1H), 7.28 (dd, *J* = 1.8, 8.7 Hz, 1H), 7.25 (d, *J* = 1.8 Hz, 1H), 7.15 (dd, *J* = 8.7, 1.8 Hz, 1H), 7.08 (d, *J* = 2.1 Hz, 1H), 6.68 (d, *J* = 8.7

Hz, 1H), 4.48–4.52 (m, 2H), 4.51 (d, *J* = 17.7 Hz, 1H), 4.45 (d, *J* = 17.7 Hz, 1H), 3.90 (s, 3H), 3.80 (s, 3H), 3.55–3.60 (m, 2H), 3.40–3.55 (m, 2H), 2.95–3.05 (m, 1H), 2.68–2.75 (m, 1H). MS *m/z* 608.4 (M + H⁺).

4-[[[6-Cyano-1-(3-methyl-3*H*-imidazol-4-ylmethyl)-1,2,3,4-tetrahydro-quinolin-3-yl]-(1,5-dimethyl-1*H*-imidazole-4-sulfonyl)-aminol-methyl]-piperidine-1-carboxylic Acid Methyl Ester (234). ¹H NMR (300 MHz, methanol-*d*₄) δ 8.93 (s, 1H), 7.73 (s, 1H), 7.40 (s, 1H), 7.37 (dd, *J* = 3.0, 9.0 Hz, 1H), 7.32 (d, *J* = 1.8 Hz, 1H), 6.79 (d, *J* = 9 Hz, 1H), 4.81 (d, *J* = 18.0 Hz, 1H), 4.68 (d, *J* = 18.0 Hz, 1H), 4.32–4.42 (m, 1H), 4.08–4.18 (m, 2H), 3.92 (s, 3H), 3.67 (s, 3H), 3.68 (s, 3H), 3.51–3.58 (m, 2H), 2.98–3.17 (m, 3H), 2.73–2.87 (m, 3H), 2.48 (s, 3H), 1.69–1.85, (m, 3H), 1.01–1.27 (m, 2H). MS *m/z* 581.6 (M + H⁺).

4-[[[6-Cyano-1-(3-methyl-3*H*-imidazol-4-ylmethyl)-1,2,3,4-tetrahydro-quinolin-3-yl]-(1,5-dimethyl-1*H*-imidazole-4-sulfonyl)-aminol-methyl]-piperidine-1-carboxylic Acid *tert*-Butyl Ester (235). ¹H NMR (300 MHz, methanol-*d*₄) δ 8.93 (s, 1H), 7.73 (s, 1H), 7.43 (d, *J* = 1.8 Hz, 1H), 7.37 (dd, *J* = 3, 9 Hz, 1H), 7.32 (s, 1H), 6.79 (s, 1H), 4.81 (d, *J* = 18.0 Hz, 1H), 4.68 (d, *J* = 18.0 Hz, 1H), 4.33–4.40 (m, 1H), 4.06–4.11 (m, 2H), 3.92 (s, 3H), 3.67 (s, 3H), 3.53–3.58 (m, 2H), 3.09–3.17 (m, 3H), 2.64–2.81 (m, 3H), 2.48 (s, 3H), 1.63–1.81 (m, 3H), 1.4 (s, 9H), 0.90–1.13 (m, 2H). MS *m/z* 623.6 (M + H⁺).

1-Methyl-1*H*-imidazole-4-sulfonic Acid [6-Cyano-1-(3-methyl-3*H*-imidazol-4-ylmethyl)-1,2,3,4-tetrahydro-quinolin-3-yl]-[2-(2-oxo-pyrrolidin-1-yl)-ethyl]-amide (117). ¹H NMR (300 MHz, methanol-*d*₄) δ 8.91 (s, 1H), 7.30–7.45 (m, 2H), 7.17–7.24 (m, 1H), 7.12 (s, 1H), 6.82 (d, *J* = 9.0 Hz, 1H), 6.52 (d, *J* = 9.0 Hz, 1H), 4.28–4.40 (m, 2H), 3.93 (s, 3H), 3.80 (s, 3H), 3.66–3.73 (m, 1H), 3.51–3.63 (m, 2H), 3.40–3.48 (m, 2H), 3.03–3.21 (m, 2H), 2.78–2.93 (m, 2H), 2.62–2.76 (m, 2H), 2.38 (t, *J* = 6.0 Hz, 2H), 2.07 (t, *J* = 6.0 Hz, 2H). MS *m/z* 523.3 (M + H⁺).

1,5-Dimethyl-1*H*-imidazole-4-sulfonic Acid [6-Cyano-1-(3-methyl-3*H*-imidazol-4-ylmethyl)-1,2,3,4-tetrahydro-quinolin-3-yl]-(4-methanesulfonyl-benzyl)-amide (236). ¹H NMR (300 MHz, methanol-*d*₄) δ 8.85 (s, 1H), 7.91 (d, *J* = 9.0 Hz, 2H), 7.77 (s, 1H), 7.60 (d, *J* = 9.0 Hz, 2H), 7.35 (d, *J* = 9.0 Hz, 2H), 7.29 (s, 1H), 6.68 (d, *J* = 9.0 Hz, 1H), 4.40–4.71 (m, 5H), 3.83 (s, 3H), 3.68 (s, 3H), 3.45–3.55 (m, 2H), 3.17 (s, 3H), 2.88–3.02 (m, 2H), 2.42 (s, 3H). MS *m/z* 594.5 (M + H⁺).

1,5-Dimethyl-1*H*-imidazole-4-sulfonic Acid [6-Cyano-1-(3-methyl-3*H*-imidazol-4-ylmethyl)-1,2,3,4-tetrahydro-quinolin-3-yl]-(4-ethanesulfonyl-benzyl)-amide (237). ¹H NMR (300 MHz, methanol-*d*₄) δ 8.88 (s, 1H), 7.85 (d, *J* = 9.0 Hz, 2H), 7.78 (s, 1H), 7.60 (d, *J* = 9.0 Hz, 2H), 7.35 (d, *J* = 9.0 Hz, 2H), 7.29 (s, 1H), 6.68 (d, *J* = 9.0 Hz, 1H), 4.40–4.76 (m, 5H), 3.97 (s, 3H), 3.82 (s, 3H), 3.45–3.55 (m, 2H), 3.15–3.30 (m, 2H), 2.88–3.05 (m, 2H), 2.48 (s, 3H), 1.22 (t, *J* = 9.6 Hz, 3H). MS *m/z* 608.4 (M + H⁺).

1,5-Dimethyl-1*H*-imidazole-4-sulfonic Acid (5-Bromo-2-fluoro-benzyl)-[6-cyano-1-(3-methyl-3*H*-imidazol-4-ylmethyl)-1,2,3,4-tetrahydro-quinolin-3-yl]-amide (238). ¹H NMR (300 MHz, methanol-*d*₄) δ 8.92 (s, 1H), 7.76 (s, 1H), 7.53 (m, 1H), 7.31–7.45 (m, 3H), 7.28 (s, 1H), 6.99 (d, *J* = 9.0 Hz, 1H), 6.72 (d, *J* = 9.0 Hz, 1H), 4.42–4.75 (m, 5H), 3.89 (s, 3H), 3.67 (s, 3H), 3.50–3.62 (m, 2H), 2.95–3.10 (m, 2H), 2.40 (s, 3H). MS *m/z* 612.8 (M + H⁺).

1-Methyl-1*H*-imidazole-4-sulfonic Acid [6-Cyano-1-(3-methyl-3*H*-imidazol-4-ylmethyl)-1,2,3,4-tetrahydro-quinolin-3-yl]-(4-methanesulfonyl-benzyl)-amide (131). ¹H NMR (300 MHz, methanol-*d*₄) δ 9.0 (s, 1H), 7.95–7.85 (m, 3H), 7.60 (d, *J* = 8.7 Hz, 2H), 7.35 (t, *J* = 7.8 Hz, 3H), 7.29 (s, 1H), 6.70 (d, *J* = 8.7 Hz, 1H), 4.60–4.40 (m, 4H), 4.40–4.30 (m, 1H), 3.85 (s, 3H), 3.80 (s, 3H), 3.40–3.30 (m, 2H), 3.0–2.90 (m, 1H), 2.83–2.75 (m, 1H), 2.50 (s, 3H). MS *m/z* 580.5 (M + H⁺).

1-Methyl-1*H*-imidazole-4-sulfonic Acid [6-Cyano-1-(3-methyl-3*H*-imidazol-4-yl-methyl)-1,2,3,4-tetrahydro-quinolin-3-yl]-(3-methoxy-propyl)-amide (91). ¹H NMR (300 MHz, methanol-*d*₄) δ 8.92 (s, 1H), 7.80 (s, 1H), 7.75 (s, 1H), 7.43 (s, 1H), 7.39 (d, *J* = 8.7 Hz, 1H), 7.32 (s, 1H), 6.81 (d, *J* = 8.7 Hz, 1H), 4.78 (d, *J*

= 16.7 Hz, 1H), 4.69 (d, $J = 16.7$ Hz, 1H), 4.45–4.38 (m, 1H), 3.92 (s, 3H), 3.81 (s, 3H), 3.59–3.51 (m, 2H), 3.43–3.38 (m, 2H), 3.32 (s, 3H), 3.28–3.20 (m, 2H), 3.12–3.07 (m, 1H), 2.85 (dd, $J = 3.3, 15.3$ Hz, 1H), 1.96–1.85 (m, 4H). MS m/z 484.5 (M + H⁺).

1-Methyl-1H-imidazole-4-sulfonic Acid [6-Cyano-1-(3-methyl-3H-imidazol-4-ylmethyl)-1,2,3,4-tetrahydro-quinolin-3-yl]-(5-trifluoromethyl-furan-2-ylmethyl)-amide (108). ¹H NMR (300 MHz, methanol-*d*₄) δ 8.90 (s, 1H), 7.72 (s, 1H), 7.60 (s, 1H), 7.42–7.36 (m, 2H), 7.40 (s, 1H), 6.90 (s, 1H), 6.70 (d, $J = 8.5$ Hz, 1H), 6.50 (s, 1H), 4.75–4.45 (m, 5H), 3.90 (s, 3H), 3.75 (s, 3H), 3.50–3.40 (m, 2H), 3.20–3.12 (m, 1H), 2.89 (dd, $J = 3.2, 15.1$ Hz, 1H). MS m/z 560.4 (M + H⁺).

1-Methyl-1H-imidazole-4-sulfonic Acid [6-Cyano-1-(3-methyl-3H-imidazol-4-ylmethyl)-1,2,3,4-tetrahydro-quinolin-3-yl]-[4-(1,3-dioxo-1,3-dihydro-isoindol-2-ylloxy)-butyl]-amide (143). ¹H NMR (300 MHz, methanol-*d*₄) δ 8.90 (s, 1H), 7.78–7.65 (m, 6H), 7.60 (s, 1H), 7.40–7.30 (m, 2H), 6.80 (d, $J = 8.7$ Hz, 1H), 4.85 (d, $J = 16.7$ Hz, 1H), 4.75 (d, $J = 16.7$ Hz, 1H), 4.50–4.40 (m, 1H), 4.20 (t, 2H), 4.0 (s, 3H), 3.80 (s, 3H), 3.70–3.55 (m, 2H), 3.40–3.20 (m, 3H), 2.89 (dd, $J = 3.2, 15.1$ Hz, 1H), 1.96–1.70 (m, 4H). MS (EI) m/z 629.6 (M + H⁺).

General Procedure for the Synthesis of Compounds According to Scheme 2. Compound **6** (400 mg) was dissolved in dichloromethane (5 mL), and trifluoroacetic acid (1 mL) was added. The reaction mixture was stirred for 45 min. Solvent was removed in vacuo with care to be sure that all trifluoroacetic acid was removed. The residue was used without further purification.

The residue (0.28 mmol) was dissolved in dichloromethane (2.5 mL) together with diisopropylethyl amine (0.33 mmol). To this solution was added the appropriate chloroformate, isocyanate, or sulfonyl chloride (0.30 mmol) dropwise at 0 °C, and the mixture was stirred for 1 h. Aqueous NH₄OH (1 mL) was added to the reaction mixture. After being stirred for an additional 15 min, the mixture was diluted with ethyl acetate (50 mL) and washed with brine. The organic layer was dried over MgSO₄ and evaporated under reduced pressure to yield the crude product, which was purified by preparative HPLC. The appropriate fractions were combined and concentrated in vacuo to give the corresponding derivatives as the trifluoroacetate salt.

Pyridine-2-sulfonic Acid [6-Cyano-1-(3-methyl-3H-imidazol-4-ylmethyl)-1,2,3,4-tetrahydro-quinolin-3-yl]-piperidin-4-ylmethylamide (54). ¹H NMR (300 MHz, methanol-*d*₄) δ 8.93 (s, 1H), 8.71 (d, $J = 7.2$ Hz, 1H), 8.07 (td, $J = 1.5, 7.5$ Hz, 1H), 8.01 (dt, $J = 0.9, 7.8$ Hz, 1H), 7.66 (ddd, $J = 1.5, 4.8, 7.5$ Hz, 1H), 7.40 (s, 1H), 7.37 (d, $J = 2.1$ Hz, 1H), 7.33 (s, 1H), 6.79 (d, $J = 8.7$ Hz, 1H), 4.80 (d, $J = 17.4$ Hz, 1H), 4.65 (d, $J = 17.4$ Hz, 1H), 4.33–4.44 (m, 1H), 3.91 (s, 3H), 3.63 (t, $J = 10.8$ Hz, 1H), 3.40–3.54 (m, 4H), 3.14–3.23 (m, 2H), 2.82–3.02 (m, 3H), 1.97–2.09 (m, 3H), 1.30–1.52 (m, 2H). MS m/z 506.5 (M + H⁺).

4-[[[6-Cyano-1-(3-methyl-3H-imidazol-4-ylmethyl)-1,2,3,4-tetrahydro-quinolin-3-yl]-(pyridine-2-sulfonyl)-amino]-methyl]-piperidine-1-carboxylic Acid Methyl Ester (162). ¹H NMR (300 MHz, methanol-*d*₄) δ 8.94 (d, $J = 0.9$ Hz, 1H), 8.70 (d, $J = 7.5$ Hz, 1H), 8.08 (td, $J = 1.8, 7.8$ Hz, 1H), 8.0 (dt, $J = 1.2, 7.8$ Hz, 1H), 7.66 (ddd, $J = 1.5, 4.8, 7.5$ Hz, 1H), 7.43 (d, $J = 1.2$ Hz, 1H), 7.38 (dd, $J = 2.1, 8.7$ Hz, 1H), 7.33 (s, 1H), 6.81 (d, $J = 8.7$ Hz, 1H), 4.84 (d, $J = 17.7$ Hz, 1H), 4.68 (d, $J = 17.7$ Hz, 1H), 4.38–4.51 (m, 1H), 4.08–4.16 (m, 2H), 3.92 (s, 3H), 3.65 (s, 3H), 3.51–3.62 (m, 2H), 3.21–3.26 (m, 2H), 3.11–3.18 (m, 1H), 2.79–2.87 (m, 3H), 1.68–1.88 (m, 3H), 1.05–1.17 (m, 2H). MS m/z 564.4 (M + H⁺).

4-[[[6-Cyano-1-(3-methyl-3H-imidazol-4-ylmethyl)-1,2,3,4-tetrahydro-quinolin-3-yl]-(pyridine-2-sulfonyl)-amino]-methyl]-piperidine-1-carboxylic Acid Isobutyl Ester (167). ¹H NMR (300 MHz, methanol-*d*₄) δ 8.94 (d, $J = 0.9$ Hz, 1H), 8.70 (d, $J = 7.5$ Hz, 1H), 8.08 (td, $J = 1.8, 7.8$ Hz, 1H), 8.0 (dt, $J = 1.2, 7.8$ Hz, 1H), 7.66 (ddd, $J = 1.5, 4.8, 7.5$ Hz, 1H), 7.43 (d, $J = 1.2$ Hz, 1H), 7.38 (dd, $J = 2.1, 8.7$ Hz, 1H), 7.33 (s, 1H), 6.81 (d, $J = 8.7$ Hz, 1H), 4.84 (d, $J = 17.7$ Hz, 1H), 4.68 (d, $J = 17.7$ Hz, 1H), 4.38–4.51 (m, 1H), 4.08–4.16 (m, 2H), 3.92 (s, 3H), 3.85 (d, $J =$

6.6 Hz, 2H), 3.51–3.62 (m, 2H), 3.21–3.26 (m, 2H), 3.11–3.18 (m, 1H), 2.79–2.87 (m, 3H), 1.91–1.99 (m, 1H), 1.68–1.88 (m, 3H), 1.05–1.17 (m, 2H), 0.95 (d, $J = 6.9$ Hz, 6H). MS m/z 606.5 (M + H⁺).

Pyridine-2-sulfonic Acid [6-Cyano-1-(3-methyl-3H-imidazol-4-ylmethyl)-1,2,3,4-tetrahydro-quinolin-3-yl]-[1-(2,2-dimethylpropionyl)-piperidin-4-ylmethyl]-amide (150). ¹H NMR (500 MHz, methanol-*d*₄) δ 8.94 (s, 1H), 8.71 (d, $J = 6$ Hz, 1H), 8.09 (td, $J = 1, 8$ Hz, 1H), 8.01 (dt, $J = 1, 8$ Hz, 1H), 7.66 (ddd, $J = 1.5, 5, 7.5$ Hz, 1H), 7.43 (s, 1H), 7.38 (dd, $J = 2, 8$ Hz, 1H), 7.33 (s, 1H), 6.82 (d, $J = 9$ Hz, 1H), 4.82 (d, $J = 18.5$ Hz, 1H), 4.69 (d, $J = 18.5$ Hz, 1H), 4.38–4.45 (m, 3H), 3.92 (s, 3H), 3.61–3.66 (m, 1H), 3.52–3.55 (m, 1H), 3.15–3.30 (m, 3H), 2.76–2.88 (m, 3H), 1.93–1.97 (m, 1H), 1.77–1.85 (m, 2H), 1.27 (s, 9H), 1.07–1.15 (m, 2H). MS m/z 590.6 (M + H⁺).

Pyridine-2-sulfonic Acid [6-Cyano-1-(3-methyl-3H-imidazol-4-ylmethyl)-1,2,3,4-tetrahydro-quinolin-3-yl]-[1-(3,3,3-trifluoropropionyl)-piperidin-4-ylmethyl]-amide (155). ¹H NMR (300 MHz, methanol-*d*₄) δ 8.85 (s, 1H), 8.67 (d, $J = 6$ Hz, 1H), 8.09 (td, $J = 1, 8$ Hz, 1H), 8.01 (dt, $J = 1, 8$ Hz, 1H), 7.60 (m, 1H), 7.43 (s, 1H), 7.38 (d, $J = 8$ Hz, 1H), 7.23 (s, 1H), 6.82 (d, $J = 9$ Hz, 1H), 4.82 (d, $J = 18.5$ Hz, 1H), 4.69 (d, $J = 18.5$ Hz, 1H), 4.38–4.45 (m, 3H), 3.92 (s, 3H), 3.61–3.66 (m, 1H), 3.50–3.52 (m, 1H), 3.12–3.28 (m, 5H), 2.71–2.81 (m, 3H), 1.93–1.97 (m, 1H), 1.72–1.80 (m, 2H), 1.03–1.12 (m, 2H). MS m/z 616.4 (M + H⁺).

Pyridine-2-sulfonic Acid [6-Cyano-1-(3-methyl-3H-imidazol-4-ylmethyl)-1,2,3,4-tetrahydro-quinolin-3-yl]-(1-methanesulfonyl-piperidin-4-ylmethyl)-amide (177). ¹H NMR (300 MHz, methanol-*d*₄) δ 8.93 (d, $J = 1.2$ Hz, 1H), 8.71 (d, $J = 7.5$ Hz, 1H), 8.08 (dt, $J = 1.8, 7.8$ Hz, 1H), 8.02 (td, $J = 1.2, 8.1$ Hz, 1H), 7.66 (ddd, $J = 1.5, 4.8, 7.5$ Hz, 1H), 7.42 (d, $J = 1.5$ Hz, 1H), 7.38 (dd, $J = 2.1, 8.7$ Hz, 1H), 7.33 (s, 1H), 6.80 (d, $J = 8.7$ Hz, 1H), 4.8 (d, $J = 17.7$ Hz, 1H), 4.68 (d, $J = 17.7$ Hz, 1H), 4.37–4.48 (m, 1H), 3.91 (s, 3H), 3.69–3.72 (m, 2H), 3.58–3.65 (m, 1H), 3.49–3.55 (m, 1H), 3.22–3.28 (m, 2H), 3.13–3.20 (m, 1H), 2.85–2.89 (m, 1H), 2.82 (s, 3H), 2.64–2.74 (m, 2H), 1.75–1.93 (m, 3H), 1.17–1.35 (m, 2H). MS m/z 584.4 (M + H⁺).

Pyridine-2-sulfonic Acid (1-Benzenesulfonyl-piperidin-4-ylmethyl)-[6-cyano-1-(3-methyl-3H-imidazol-4-ylmethyl)-1,2,3,4-tetrahydro-quinolin-3-yl]-amide (180). ¹H NMR (300 MHz, methanol-*d*₄) δ 8.93 (d, $J = 1.2$ Hz, 1H), 8.71 (d, $J = 7.5$ Hz, 1H), 8.08 (dt, $J = 1.8, 7.8$ Hz, 1H), 8.02 (td, $J = 1.2, 8.1$ Hz, 1H), 7.56–7.78 (m, 6H), 7.32 (s, 1H), 7.29 (d, $J = 8.7$ Hz, 1H), 7.21 (s, 1H), 6.80 (d, $J = 8.7$ Hz, 1H), 4.75 (d, $J = 17.7$ Hz, 1H), 4.60 (d, $J = 17.7$ Hz, 1H), 4.37–4.48 (m, 1H), 3.91 (s, 3H), 3.69–3.72 (m, 2H), 3.58–3.65 (m, 1H), 3.49–3.55 (m, 1H), 3.22–3.28 (m, 2H), 3.13–3.20 (m, 1H), 2.85–2.89 (m, 1H), 2.64–2.74 (m, 2H), 1.75–1.93 (m, 3H), 1.17–1.35 (m, 2H). MS m/z 646.5 (M + H⁺).

4-[[[6-Cyano-1-(3-methyl-3H-imidazol-4-ylmethyl)-1,2,3,4-tetrahydro-quinolin-3-yl]-(pyridine-2-sulfonyl)-amino]-methyl]-piperidine-1-carboxylic Acid Ethylamide (170). ¹H NMR (300 MHz, methanol-*d*₄) δ 8.93 (s, 1H), 8.70 (d, $J = 7.2$ Hz, 1H), 8.04–8.10 (m, 1H), 8.99–8.02 (m, 1H), 7.66 (ddd, $J = 1.5, 4.8, 7.5$ Hz, 1H), 7.42 (s, 1H), 7.39 (dd, $J = 2.1, 8.4$ Hz, 1H), 7.33 (s, 1H), 6.82 (d, $J = 8.7$ Hz, 1H), 4.8 (d, $J = 17.7$ Hz, 1H), 4.69 (d, $J = 17.7$ Hz, 1H), 4.38–4.47 (m, 1H), 3.98–4.02 (m, 2H), 3.91 (s, 3H), 3.62 (t, $J = 10.8$ Hz, 1H), 3.54–3.56 (m, 1H), 3.12–3.29 (m, 5H), 2.81–2.90 (m, 1H), 2.66–2.74 (m, 2H), 1.65–1.87 (m, 3H), 1.17–1.18 (m, 2H), 1.10 (t, $J = 7.2$ Hz, 3H). MS m/z 577.5 (M + H⁺).

[2-(4-[[[6-Cyano-1-(3-methyl-3H-imidazol-4-ylmethyl)-1,2,3,4-tetrahydro-quinolin-3-yl]-(pyridine-2-sulfonyl)-amino]-methyl]-piperidin-1-yl)-2-oxo-ethyl]-carbamic Acid *tert*-Butyl Ester (157). A mixture of **54** (22 mg, 0.044 mmol), Boc-Gly-OH (9.2 mg, 0.051 mmol), dicyclohexylcarbodiimide (10 mg, 0.051 mmol), 4-dimethylamino-pyridine (2 mg), and dichloromethane (5 mL) was stirred at room temperature for 18 h. Upon completion of reaction, the mixture was filtered to remove dicyclohexylurea, and the residue was washed with dichloromethane (5 mL). The filtrate and washings

were combined and evaporated to dryness *in vacuo*. The residue was purified by HPLC to afford 15 mg (54%) of **157** as the trifluoroacetate salt. $^1\text{H NMR}$ (500 MHz, methanol- d_4) δ 8.94 (s, 1H), 8.71 (d, $J = 7.5$ Hz, 1H), 8.06–8.12 (m, 1H), 7.88–8.01 (m, 1H), 7.65–7.68 (m, 1H), 7.42 (s, 1H), 7.38 (dd, $J = 1.5, 8.5$ Hz, 1H), 7.33 (s, 1H), 6.81 (d, $J = 8$ Hz, 1H), 4.81 (d, $J = 18$ Hz, 1H), 4.69 (d, $J = 18$ Hz, 1H), 4.35–4.50 (m, 3H), 3.92 (s, 3H), 3.80–3.92 (m, 2H), 3.59–3.63 (m, 1H), 3.52–3.54 (m, 1H), 3.13–3.33 (m, 3H), 3.00–3.12 (m, 1H), 2.82–2.88 (m, 1H), 2.57–2.65 (m, 1H), 1.72–1.95 (m, 3H), 1.46 (s, 9 H), 1.06–1.25 (m, 2H). MS m/z 663.6 (M + H $^+$).

General Procedure for the Synthesis of Compounds According to Scheme 3. To a solution of 6-cyano-1,2,3,4-tetrahydroquinolin-3-ylamine hydrochloride **3** (4.18 g, 20 mmol) and *N,N*-diisopropylethyl amine (5.1 g, 40 mmol) in 25 mL of anhydrous dichloromethane was added benzyl chloroformate (5.1 g, 30 mmol) at 0 °C. After stirring at ambient temperature for 5 h, the reaction mixture was quenched with water. The mixture was partitioned between water and ethyl acetate. The organic layer was washed with brine, dried over sodium sulfate, and evaporated under reduce pressure. Purification by flash chromatography gave **9** (5.49 g 89%) as a white foam.

To a solution of **9** (5 g, 16.2 mmol) and trifluoroacetic acid (14 mL) in 20 mL of dichloroethane (14 mL) at room temperature under nitrogen was added 3-methyl-3*H*-imidazole-4-carboxaldehyde (5.37 g, 48.6 mmol). The mixture was stirred for 1 h at room temperature, and then triethylsilane (7.75 mL, 48.6 mmol) was added dropwise. The mixture was heated in an oil bath at 45 °C for 15 h. The volatile materials were removed under vacuum. The reaction mixture was diluted with ethyl acetate and washed with aqueous NaHCO₃, water, and brine solution. The organic layer was dried over MgSO₄, filtered, and concentrated. The crude residue was purified on a flash silica column to afford **10** (3.1 g, 47%).

A solution of [6-cyano-1-(3-methyl-3*H*-imidazol-4-ylmethyl)-1,2,3,4-tetrahydroquinolin-3-yl]-carbamic acid benzyl ester **10** (1.3 g, 3 mmol), 15 mL methanol, and 10% Pd/C catalyst (0.5 g) was stirred under atmospheric pressure of hydrogen for 4 h. The catalyst was filtered off, and the filtrate was concentrated to give **11** as an off-white foam (790 mg, 92%).

To a suspension of **11** (0.55 g, 0.2 mmol) and Cs₂CO₃ (1.34 g, 0.4 mmol) in dry DMF (3 mL) was added the appropriate alkyl halide (0.2 mmol), and the mixture was stirred at room temperature overnight under argon. After addition of water (10 mL), the solution was extracted with ethyl acetate (3 × 10 mL). The organic layer was extracted with brine (3 × 10 mL). The combined organic layers were dried over MgSO₄ and evaporated under reduce pressure. The residue was purified by HPLC. Appropriate fractions were collected, and the pure product **12** was obtained as the TFA salt.

Compound **12** (0.1 mmol) dissolved in dichloromethane (1.5 mL) together with *N,N*-diisopropylethyl amine (0.2 mmol) was cooled to 0 °C. Acetyl chloride or sulfonyl chloride (0.12 mmol) dissolved in dichloromethane (0.5 mL) was added dropwise, and the mixture was stirred for 1 h. Aqueous NH₄OH (1 mL) was added to the reaction mixture. After being stirred for an additional 15 min, the reaction mixture was diluted with ethyl acetate (50 mL) and washed with brine solution. The organic layer was dried over MgSO₄ and evaporated under reduced pressure, yielding the crude amide **13**, which was purified by HPLC. The appropriate fractions were combined, concentrated *in vacuo*, and lyophilized to give the corresponding compounds as the trifluoroacetate salt.

(6-Cyano-1,2,3,4-tetrahydroquinolin-3-yl)-carbamic Acid Benzyl Ester (9). $^1\text{H NMR}$ (300 MHz, methanol- d_4) δ 7.02–7.15 (m, 7H), 6.58 (d, $J = 8$ Hz, 1H), 5.09 (s, 2H), 3.94–3.98 (m, 1H), 3.45 (m, 1H), 3.20 (m, 1H), 2.99 (dd $J = 4.2, 16.5$ Hz, 1H), 2.74 (ddd, $J = 2.1, 4.8, 16.5$ Hz, 1H). MS m/z 308.2 (M + H $^+$).

[6-Cyano-1-(3-methyl-3*H*-imidazol-4-ylmethyl)-1,2,3,4-tetrahydroquinolin-3-yl]-carbamic Acid Benzyl Ester (10). $^1\text{H NMR}$ (300 MHz, CD₃OD) δ 7.61 (s, 1H), 7.31–7.38 (m, 7H) 6.87 (d, $J = 8.7$ Hz, 1H), 6.83 (s, 1H), 5.07 (s, 2H), 4.59 (s, 2H), 4.00–4.02 (m, 1H), 3.64 (s, 3H), 3.36 (dd, $J = 2.7, 12$ Hz, 1H), 3.23

(dd, $J = 4.5, 12.1$ Hz, 1H), 2.03 (dd $J = 5.1, 15.9$ Hz, 1H), 2.71 (dd, $J = 4.8, 16.2$ Hz, 1H). MS m/z 402.2 (M + H $^+$).

3-Amino-1-(3-methyl-3*H*-imidazol-4-ylmethyl)-1,2,3,4-tetrahydroquinoline-6-carbonitrile (11). $^1\text{H NMR}$ (300 MHz, methanol- d_4) δ 7.61 (s, 1H), 7.32 (dd, $J = 2.1, 8.4$ Hz, 1H), 7.29 (s, 1H), 6.83 (d, $J = 8.4$ Hz, 1H), 6.80 (s, 1H), 4.64 (d, $J = 16.5$ Hz, 1H), 4.58 (d, $J = 16.5$ Hz, 1H), 3.57 (s, 3H), 3.42 (dd, $J = 2.4, 11.7$ Hz, 1H), 3.35 (m, 1H), 3.21 (m, 1H), 2.98 (dd, $J = 4.1, 16.5$ Hz, 1H), 2.67 (dd, $J = 4.8, 16.4$ Hz, 1H). MS m/z 268.3 (M + H $^+$).

3-(2-Fluoro-benzylamino)-1-(3-methyl-3*H*-imidazol-4-ylmethyl)-1,2,3,4-tetrahydroquinoline-6-carbonitrile Trifluoroacetate Salt (12). $^1\text{H NMR}$ (300 MHz, methanol- d_4) δ 8.83 (s, 1H), 7.20–7.48 (m, 5H), 7.12–7.17 (m, 2H), 6.82 (d, $J = 8.5$ Hz, 1H), 4.74 (d, $J = 17.4$ Hz, 1H), 4.60 (d, $J = 17.4$ Hz, 1H), 4.35 (s, 2H), 3.88 (m, 1H), 3.75 (s, 3H), 3.74 (dd, $J = 2.1, 14.1$ Hz, 1H), 3.49 (dd, $J = 4.8, 14.5$ Hz, 1H), 3.31 (dd, $J = 4.5, 16.5$ Hz, 1H), 2.67 (dd, $J = 6.6, 16.5$ Hz, 1H). MS m/z 268.3 (M + H $^+$).

4-[[6-Cyano-1-(3-methyl-3*H*-imidazol-4-ylmethyl)-1,2,3,4-tetrahydroquinolin-3-ylamino]-methyl]-piperidine-1-carboxylic Acid Methyl Ester (12). $^1\text{H NMR}$ (300 MHz, methanol- d_4) δ 8.87 (s, 1H), 7.43 (s, 1H), 7.38 (dd, $J = 2.1, 8.7$ Hz, 1H), 7.33 (s, 1H), 6.81 (d, $J = 8.7$ Hz, 1H), 4.84 (d, $J = 17.7$ Hz, 1H), 4.68 (d, $J = 17.7$ Hz, 1H), 3.89–4.08 (m, 3H), 3.82 (s, 3H), 3.65 (s, 3H), 3.51–3.62 (m, 2H), 3.21–3.26 (m, 2H), 3.11–3.18 (m, 1H), 2.79–2.87 (m, 3H), 1.68–1.88, (m, 3H), 1.05–1.17 (m, 2H). MS m/z 423.4 (M + H $^+$).

***N*-[6-Cyano-1-(3-methyl-3*H*-imidazol-4-ylmethyl)-1,2,3,4-tetrahydroquinolin-3-yl]-*N*-(2-fluoro-benzyl)-4-methoxy-benzene-sulfonamide (215).** $^1\text{H NMR}$ (300 MHz, methanol- d_4) δ 8.91 (s, 1H), 7.83 (d, $J = 9.1$ Hz, 2H), 7.49–7.52 (m, 1H), 7.28–7.33 (m, 3H), 7.16–7.19 (m, 2H), 7.1 (d, $J = 9.0$ Hz, 2H), 6.96–7.03 (m, 1H), 6.71 (d, $J = 9.0$ Hz, 1H), 4.30–4.61 (m, 5H), 3.91 (s, 3H), 3.81 (s, 3H), 3.30–3.39 (m, 2H), 2.94–3.04 (m, 1H), 2.75 (dd, $J = 4.8, 15.6$ Hz, 1H). MS m/z 546.5 (M + H $^+$).

1-Methyl-1*H*-pyrazole-4-sulfonic Acid [6-Cyano-1-(3-methyl-3*H*-imidazol-4-ylmethyl)-1,2,3,4-tetrahydroquinolin-3-yl]-(2-fluoro-benzyl)-amide (213). $^1\text{H NMR}$ (300 MHz, methanol- d_4) δ 8.91 (s, 1H), 8.19 (s, 1H), 7.82 (s, 1H), 7.56–7.61 (m, 1H), 7.27–7.36 (m, 4H), 7.14–7.22 (m, 1H), 7.01–7.09 (m, 1H), 6.72 (d, $J = 8.4$ Hz, 1H), 4.32–4.59 (m, 5H), 3.96 (s, 3H), 3.82 (s, 3H), 3.30–3.39 (m, 2H), 3.03–3.12 (m, 1H), 2.86 (dd, $J = 4.8, 15.6$ Hz, 1H). MS m/z 520.4 (M + H $^+$).

3-Methyl-3*H*-imidazole-4-sulfonic Acid [6-Cyano-1-(3-methyl-3*H*-imidazol-4-ylmethyl)-1,2,3,4-tetrahydroquinolin-3-yl]-(4-methanesulfonyl-benzyl)-amide (221). $^1\text{H NMR}$ (300 MHz, methanol- d_4) δ 8.89 (s, 1H), 7.93 (d, $J = 8.2$ Hz, 2H), 7.83 (s, 1H), 7.76 (s, 1H), 7.62 (d, $J = 8.4$ Hz, 2H), 7.31–7.35 (m, 2H), 7.26 (s, 1H), 6.68 (d, $J = 8.7$ Hz, 1H), 4.39–4.68 (m, 5H), 3.81 (s, 6H), 3.40–3.46 (m, 2H), 3.15 (s, 3H), 3.03–3.11 (m, 1H), 2.86 (m, 1H). MS m/z 580.5 (M + H $^+$).

***N*-[6-Cyano-1-(3-methyl-3*H*-imidazol-4-ylmethyl)-1,2,3,4-tetrahydroquinolin-3-yl]-*N*-(4-methanesulfonyl-benzyl)-benzene-sulfonamide (218).** $^1\text{H NMR}$ (300 MHz, methanol- d_4) δ 8.91 (s, 1H), 7.92–7.96 (m, 4H), 7.67–7.72 (m, 5H), 7.31 (dd, $J = 2.1, 8.4$ Hz, 1H), 7.27 (s, 1H), 7.16 (s, 1H), 6.63 (d, $J = 8.4$ Hz, 1H), 4.35–4.70 (m, 5H), 3.82 (s, 3H), 3.41–3.46 (m, 2H), 3.17 (s, 3H), 2.95–3.05 (m, 1H), 2.79–2.82 (m, 1H). MS m/z 576.6 (M + H $^+$).

4-[[6-Cyano-1-(3-methyl-3*H*-imidazol-4-ylmethyl)-1,2,3,4-tetrahydroquinolin-3-yl]-ethanesulfonyl-amino]-methyl-piperidine-1-carboxylic Acid Methyl Ester (200). $^1\text{H NMR}$ (300 MHz, methanol- d_4) δ 8.93 (s, 1H), 7.42 (s, 1H), 7.42 (s, 1H), 7.33 (dd, $J = 1.8, 8.4$ Hz, 1H), 6.82 (d, $J = 8.7$ Hz, 1H), 4.79 (d, $J = 18$ Hz, 1H), 4.70 (d, $J = 18$ Hz, 1H), 4.05–4.18 (m, 3H), 3.92 (s, 3H), 3.65 (s, 3H), 3.51–3.56 (m, 2H), 3.12–3.24 (m, 6H), 2.71–2.78 (m, 2H), 1.72–1.84 (m, 3H), 1.34 (t, $J = 7.5$ Hz, 3H), 1.05–1.14 (m, 2H). MS m/z 515.4 (M + H $^+$).

4-[[6-Cyano-1-(3-methyl-3*H*-imidazol-4-ylmethyl)-1,2,3,4-tetrahydroquinolin-3-yl]-(3-methyl-3*H*-imidazole-4-sulfonyl)-amino]-piperidine-1-carboxylic Acid Methyl Ester (191). $^1\text{H NMR}$ (300 MHz, methanol- d_4) δ 8.93 (s, 1H), 7.76 (s, 1H), 7.74 (s, 1H), 7.45 (s, 1H), 7.33 (dd, $J = 1.8, 8.4$ Hz, 1H), 7.32 (s, 1H),

6.82 (d, $J = 8.7$ Hz, 1H), 4.78 (d, $J = 17.4$ Hz, 1H), 4.70 (d, $J = 17.4$ Hz, 1H), 4.32–4.41 (m, 1H), 3.99–4.1 (m, 2H), 3.92 (s, 3H), 3.80 (s, 3H), 3.65 (s, 3H), 3.51–3.56 (2H), 2.96–3.14 (m, 4H), 2.71–2.78 (m, 2H), 1.71–1.88 (m, 3 H), 1.00–1.13 (m, 2H). MS m/z 567.5 (M + H⁺).

4-((Benzo[1,2,5]thiadiazole-4-sulfonyl)-[6-cyano-1-(3-methyl-3H-imidazol-4-ylmethyl)-1,2,3,4-tetrahydro-quinolin-3-yl]-amino)-methyl-piperidine-1-carboxylic Acid Methyl Ester (188). ¹H NMR (300 MHz, methanol-*d*₄) δ 8.94 (s, 1H), 8.32–8.35 (m, 1H), 8.32 (s, 1H), 7.08–7.85 (m, 1H), 7.42 (s, 1H), 7.35 (dd, $J = 1.8$, 8.7 Hz, 1H), 7.24 (s, 1H), 6.82 (d, $J = 8.7$ Hz, 1H), 4.78 (d, $J = 18$ Hz, 1H), 4.62 (d, $J = 18$ Hz, 1H), 4.04–4.08 (m, 3H), 3.91 (s, 3H), 3.66 (s, 3H), 3.49–3.51 (m, 3H), 3.03–3.10 (m, 2H), 2.61–2.73 (m, 3H), 1.71–1.88 (m, 3 H), 1.02–1.14 (m, 2H). MS m/z 567.5 (M + H⁺).

4-[[6-Cyano-1-(3-methyl-3H-imidazol-4-ylmethyl)-1,2,3,4-tetrahydro-quinolin-3-yl]-3,4-dihydro-2H-benzo[*b*][1,4]dioxepine-7-sulfonyl-amino]-methyl-piperidine-1-carboxylic Acid Methyl Ester (204). ¹H NMR (300 MHz, methanol-*d*₄) δ 8.94 (s, 1H), 7.45 (s, 1H), 7.39 (dd, $J = 2.1$, 8.7 Hz, 1H), 7.36 (dd, $J = 2.1$, 8.7 Hz, 1H), 7.35 (d, $J = 2.1$ Hz, 1H), 7.29 (s, 1H), 7.25 (d, $J = 8.7$ Hz, 1H), 7.10 (d, $J = 8.7$ Hz, 1H), 6.88 (d, $J = 8.7$ Hz, 1H), 4.64 (d, $J = 16.7$ Hz, 1H), 4.51 (d, $J = 16.7$ Hz, 1H), 4.24–4.33 (m, 4H), 4.04–4.14 (m, 3H), 3.85 (s, 3H), 3.64 (s, 3H), 3.16–3.19 (m, 1H), 2.99–3.03 (m, 3H), 2.63–2.80 (m, 4H), 2.21–2.29 (m, 2H), 1.68–1.78 (m, 3H), 1.00–1.06 (m, 2H). MS m/z 635.7 (M + H⁺).

4-((Benzo[1,2,5]oxadiazole-4-sulfonyl)-[6-cyano-1-(3-methyl-3H-imidazol-4-ylmethyl)-1,2,3,4-tetrahydro-quinolin-3-yl]-amino)-methyl-piperidine-1-carboxylic Acid Methyl Ester (205). ¹H NMR (300 MHz, methanol-*d*₄) δ 8.94 (s, 1H), 8.27–8.29 (m, 1H), 8.19–8.22 (m, 1H), 7.68 (s, 1H), 7.40–7.49 (m, 1H), 7.35 (dd, $J = 1.8$, 8.7 Hz, 1H), 7.29 (s, 1H), 6.82 (d, $J = 8.7$ Hz, 1H), 4.78 (d, $J = 16.7$ Hz, 1H), 4.62 (d, $J = 16.7$ Hz, 1H), 4.04–4.08 (m, 3H), 3.91 (s, 3H), 3.66 (s, 3H), 3.49–3.51 (m, 3H), 3.03–3.10 (m, 2H), 2.61–2.73 (m, 3H), 1.71–1.88 (m, 3H), 1.02–1.14 (m, 2H). MS m/z 605.4 (M + H⁺).

4-[[6-Cyano-1-(3-methyl-3H-imidazol-4-ylmethyl)-1,2,3,4-tetrahydro-quinolin-3-yl]-2-oxo-2H-chromene-6-sulfonyl-amino]-methyl-piperidine-1-carboxylic Acid Methyl Ester (206). ¹H NMR (300 MHz, methanol-*d*₄) δ 8.93 (s, 1H), 8.22 (d, $J = 2.1$ Hz, 1H), 8.07 (dd, $J = 2.1$, 8.7 Hz, 1H), 8.04 (d, $J = 9.9$ Hz, 1H), 7.53 (d, $J = 8.7$ Hz, 1H), 7.41 (d, $J = 2.1$ Hz, 1H), 7.37 (dd, $J = 2.1$, 8.7 Hz, 1H), 7.26 (s, 1H), 6.78 (d, $J = 8.7$ Hz, 1H), 6.58 (d, $J = 9.9$ Hz, 1H), 4.75 (d, $J = 16.7$ Hz, 1H), 4.68 (d, $J = 16.7$ Hz, 1H), 4.04–4.08 (m, 3H), 3.90 (s, 3H), 3.66 (s, 3H), 3.49–3.51 (m, 1H), 3.03–3.15 (m, 3H), 2.61–2.80 (m, 3H), 1.60–1.71 (m, 3H), 1.02–1.16 (m, 2H). MS m/z 631.4 (M + H⁺).

4-((4-Carboxy-furan-3-sulfonyl)-[6-cyano-1-(3-methyl-3H-imidazol-4-ylmethyl)-1,2,3,4-tetrahydro-quinolin-3-yl]-amino)-methyl-piperidine-1-carboxylic Acid Methyl Ester (197). ¹H NMR (300 MHz, methanol-*d*₄) δ 8.93 (s, 1H), 7.43 (dd, $J = 2.1$ Hz, 1H), 7.30 (d, $J = 8.7$ Hz, 1H), 7.38 (d, $J = 6.0$ Hz, 1H), 7.36 (s, 1H), 7.25 (d, $J = 6.0$ Hz, 1H), 6.83 (d, $J = 8.7$ Hz, 1H), 6.88 (d, $J = 8.7$ Hz, 1H), 4.78 (d, $J = 16.7$ Hz, 1H), 4.62 (d, $J = 16.7$ Hz, 1H), 4.08–4.04 (m, 3H), 3.91 (s, 3H), 3.66 (s, 3H), 3.49–3.51 (m, 3H), 3.03–3.10 (m, 2H), 2.61–2.73 (m, 3H), 1.71–1.88 (m, 3H), 1.02–1.14 (m, 2H). MS m/z 597.4 (M + H⁺).

4-[[6-Cyano-1-(3-methyl-3H-imidazol-4-ylmethyl)-1,2,3,4-tetrahydro-quinolin-3-yl]-methanesulfonylmethanesulfonyl-amino)-methyl-piperidine-1-carboxylic Acid Methyl Ester (207). ¹H NMR (300 MHz, methanol-*d*₄) δ 8.96 (s, 1H), 7.49 (dd, $J = 2.1$, 8.7 Hz, 1H), 7.47 (d, $J = 2.1$ Hz, 1H), 6.88 (d, $J = 8.7$ Hz, 1H), 5.15 (s, 2H), 4.68 (d, $J = 16.7$ Hz, 1H), 4.62 (d, $J = 16.7$ Hz, 1H), 4.40–4.25 (m, 1H), 4.04–4.14 (m, 2H), 3.92 (s, 3H), 3.73 (s, 3H), 3.55–3.61 (m, 3H), 3.25 (s, 3H), 3.16–3.19 (m, 1H), 2.99–3.03 (m, 2H), 2.63–2.80 (m, 2H), 2.21–2.29 (m, 1H), 1.68–1.78 (m, 2H), 1.05–1.16 (m, 2H). MS m/z 579.2 (M + H⁺).

4-((6-Cyano-1-(3-methyl-3H-imidazol-4-ylmethyl)-1,2,3,4-tetrahydro-quinolin-3-yl)-cyclopropanesulfonyl-amino)-methyl-piperidine-1-carboxylic Acid Methyl Ester (202). ¹H NMR (300 MHz, methanol-*d*₄) δ 8.94 (s, 1H), 7.52 (dd, $J = 1.8$, 8.7 Hz, 1H),

7.48 (d, $J = 2.0$ Hz), 7.42 (s, 1H), 6.85 (d, $J = 8.7$ Hz, 1H), 4.78 (d, $J = 16.7$ Hz, 1H), 4.62 (d, $J = 16.7$ Hz, 1H), 4.08–4.30 (m, 3H), 3.95 (s, 3H), 3.75 (s, 3H), 3.51–3.72 (m, 4H), 3.10–3.40 (m, 4H), 2.80–3.02 (m, 2H), 2.68–2.73 (m, 1H), 1.75–2.01 (m, 3H), 1.10–1.30 (brm, 6H). MS m/z 527.4 (M + H⁺).

3,4-Dihydro-2H-benzo[*b*][1,4]dioxepine-7-sulfonic Acid [6-Cyano-1-(3-methyl-3H-imidazol-4-ylmethyl)-1,2,3,4-tetrahydro-quinolin-3-yl]-4-methanesulfonyl-benzyl-amide (223). ¹H NMR (300 MHz, methanol-*d*₄) δ 8.94 (s, 1H), 7.87 (d, $J = 8.1$ Hz, 2H), 7.62 (d, $J = 8.1$ Hz, 2H), 7.45 (s, 1H), 7.39 (dd, $J = 2.1$, 8.7 Hz, 1H), 7.36 (dd, $J = 2.1$, 8.7 Hz, 1H), 7.35 (d, $J = 2.1$ Hz, 1H), 7.29 (s, 1H), 7.25 (d, $J = 8.7$ Hz, 1H), 7.10 (d, $J = 8.7$ Hz, 1H), 6.68 (d, $J = 8.7$ Hz, 1H), 4.64 (d, $J = 16.7$ Hz, 1H), 4.51 (d, $J = 16.7$ Hz, 1H), 4.24–4.33 (m, 4H), 4.04–4.14 (m, 2H), 3.85 (s, 3H), 3.20 (s, 3H), 2.95–3.05 (m, 1H), 1.12–1.25 (m, 2H). MS m/z 648.5 (M + H⁺).

3-Methyl-thiophene-2-sulfonic Acid [6-Cyano-1-(3-methyl-3H-imidazol-4-ylmethyl)-1,2,3,4-tetrahydro-quinolin-3-yl]-4-methanesulfonyl-benzyl-amide (224). ¹H NMR (300 MHz, methanol-*d*₄) δ 8.87 (s, 1H), 7.98 (d, $J = 8.1$ Hz, 2H), 7.72 (d, $J = 5.1$ Hz, 1H), 7.61 (dd, $J = 1.8$, 8.7 Hz, 1H), 7.35 (d, $J = 8.7$ Hz, 1H), 7.25 (m, 2H), 7.07 (d, $J = 5.1$ Hz, 1H), 6.70 (d, $J = 8.7$ Hz, 1H), 4.75 (d, 2H), 4.53–4.55 (m, 1H), 4.51 (d, $J = 17.7$ Hz, 1H), 4.48 (d, $J = 17.7$ Hz, 1H), 3.79 (s, 3H), 3.10–3.25 (m, 7H), 2.95–3.05 (m, 1H), 2.49 (s, 3H). MS m/z 596.6 (M + H⁺).

***N*-[6-Cyano-1-(3-methyl-3H-imidazol-4-ylmethyl)-1,2,3,4-tetrahydro-quinolin-3-yl]-2-dimethylamino-*N*-(2-fluoro-benzyl)-acetamide (248).** ¹H NMR (300 MHz, methanol-*d*₄) δ 8.78 (s, 1H), 7.01–7.34 (m, 7 H), 6.68 (d, $J = 8.7$ Hz, 1H), 4.42–4.61 (m, 3H), 4.25 (d, $J = 15.9$ Hz, 1H), 4.18 (d, $J = 15.9$ Hz, 1H), 3.74 (s, 3H), 3.41–3.59 (m, 2H), 3.19 (s, 2H), 2.94–3.04 (m, 1H), 2.86 (m, 7 H). MS m/z 461.3 (M + H⁺).

***N*-[6-Cyano-1-(3-methyl-3H-imidazol-4-ylmethyl)-1,2,3,4-tetrahydro-quinolin-3-yl]-*N*-(2-fluoro-benzyl)-3-methylsulfanylpropionamide (247).** ¹H NMR (300 MHz, methanol-*d*₄) δ 8.84 (s, 1H), 7.01–7.34 (m, 7H), 6.78 (d, $J = 7.6$ Hz, 1H), 4.42–4.77 (m, 5H), 3.84 (s, 3H), 3.41–3.59 (m, 2H), 2.94–3.12 (m, 6H), 2.06 (s, 3H). MS m/z 478.4 (M + H⁺).

General Procedure for the Synthesis of Compounds According to Scheme 4. 1-Methyl-1H-imidazole-4-sulfonic Acid [6-Cyano-1-(1-trityl-1H-imidazol-4-ylmethyl)-1,2,3,4-tetrahydro-quinolin-3-yl]-amide (15). A solution of **14** (0.397 g, 1 mmol), *N,N*-diisopropylethyl amine (2.37 mL, 2 mmol), and 3 mL of dry DMF was stirred at room temperature for 30 min. To this solution was added dropwise a solution of triphenylmethyl chloride (0.278 g, 1 mmol) dissolved in dry DMF (3 mL). The reaction mixture was stirred at room temperature for 20 h. After addition of water (10 mL), the solution was extracted with dichloromethane (3 \times 15 mL). The combined organic layer was washed with brine (20 mL) and the organic layer was dried over MgSO₄ and evaporated under reduce pressure, yielding the crude product, which was purified on a silica gel column eluting with 10% methanol in ethyl acetate to afford **15** (0.562 g, 88%). ¹H NMR (300 MHz, CDCl₃) δ 8.0 (s, 1H), 7.9 (s, 1H), 7.4 (s, 1H), 7.25–7.37 (m, 18 H), 6.48 (d, $J = 8.7$ Hz, 1H), 4.5 (d, $J = 16.2$ Hz, 1H), 4.23 (d, $J = 16.2$ Hz, 1H), 4.00–4.09 (m, 1H), 3.70 (s, 3H), 3.51–3.61 (m, 1H), 3.31–3.34 (m, 1H), 3.09–3.12 (m, 1H), 2.86–3.07 (m, 1H). MS m/z 640.3 (M + H⁺).

A solution of **16** (0.21 mmol), dichloromethane (3 mL), and trifluoroacetic acid (0.5 mL) was stirred for 30 min. The reaction mixture was filtered to remove trityl alcohol, and the residue was washed with dichloromethane. The filtrate and washings were combined and then evaporated to dryness via rotary evaporation. The residue was purified by HPLC.

1-Methyl-1H-imidazole-4-sulfonic Acid Benzyl-[6-cyano-1-(3H-imidazol-4-ylmethyl)-1,2,3,4-tetrahydro-quinolin-3-yl]-amide (253). ¹H NMR (300 MHz, methanol-*d*₄) δ 8.86 (s, 1H), 7.83 (s, 1H), 7.71 (s, 1H), 7.18–7.39 (m, 8 H), 6.71 (d, $J = 9.7$ Hz, 1H), 4.29–4.73 (m, 5H), 3.80 (s, 3H), 3.36–3.42 (m, 1H), 3.18–3.26 (m, 1H), 3.12 (dd, $J = 8.7$, 15.6 Hz, 1H), 2.89 (dd, $J = 3.3$, 15.3 Hz, 1H). MS m/z 488.1 (M + H⁺).

1-Methyl-1*H*-imidazole-4-sulfonic Acid (2-Bromo-allyl)-[6-cyano-1-(3*H*-imidazol-4-ylmethyl)-1,2,3,4-tetrahydro-quinolin-3-yl]-amide (252). ¹H NMR (300 MHz, methanol-*d*₄) δ 8.86 (s, 1H), 7.83 (s, 1H), 7.79 (s, 1H), 7.28 (s, 1H), 7.33 (dd, *J* = 2.1, 9.0 Hz, 1H), 7.28 (s, 1H), 6.65 (d, *J* = 8.7 Hz, 1H), 6.04 (s, 1H), 5.65 (s, 1H), 4.79 (d, *J* = 17.1 Hz, 1H), 4.62 (d, *J* = 17.1 Hz, 1H), 4.39–4.59 (m, 1H), 4.19 (d, *J* = 17.1 Hz, 1H), 4.0 (d, *J* = 17.1 Hz, 1H), 3.81 (s, 3H), 3.55–3.62 (m, 1H), 3.42–3.47 (m, 1H), 3.07–3.14 (m, 1H), 2.97 (dd, *J* = 4.5, 15.9 Hz, 1H). MS *m/z* 518.2 (M + H⁺).

Synthesis of 255 According to Scheme 5. 4-[[[6-cyano-1,2,3,4-tetrahydro-quinolin-3-yl)-(pyridine-2-sulfonyl)-amino]-methyl]-piperidine-1-carboxylic Acid Methyl Ester (18). ¹H NMR (300 MHz, methanol-*d*₄) δ 8.70 (d, *J* = 7.5 Hz, 1H), 8.08 (td, *J* = 1.8, 7.8 Hz, 1H), 8.0 (dt, *J* = 1.2, 7.8 Hz, 1H), 7.66 (ddd, *J* = 1.5, 4.8, 7.5 Hz, 1H), 7.43 (d, *J* = 1.2 Hz, 1H), 7.38 (dd, *J* = 2.1, 8.7 Hz, 1H), 6.81 (d, *J* = 8.7 Hz, 1H), 4.38–4.51 (m, 1H), 4.08–4.16 (m, 2H), 3.65 (s, 3H), 3.51–3.62 (m, 2H), 3.21–3.26 (m, 2H), 3.11–3.18 (m, 1H), 2.79–2.87 (m, 3H), 1.68–1.88 (m, 3H), 1.05–1.17 (m, 2H). MS *m/z* 470.2 (M + H⁺).

4-[[[6-Cyano-1-(3-methyl-3*H*-imidazole-4-sulfonyl)-1,2,3,4-tetrahydro-quinolin-3-yl)-(pyridine-2-sulfonyl)-amino]-methyl]-piperidine-1-carboxylic Acid Methyl Ester (255). A solution of 18 (47 mg, 0.1 mmol), 3-methyl-3*H*-imidazole-4-sulfonyl chloride hydrochloride salt (26 mg, 0.12 mmol, Apollo Scientific Intermediates), *N,N*-dimethyl pyridine (15 mg, 0.12 mmol), and 3 mL of dry acetonitrile was refluxed overnight under nitrogen. Then the reaction mixture was quenched with water and extracted with dichloromethane (3 × 10 mL). The combine organic layer was washed with brine (10 mL), and the organic layer was dried over MgSO₄ and evaporated under reduced pressure, yielding the crude product, which was purified by HPLC. ¹H NMR (300 MHz, methanol-*d*₄) δ 8.76 (d, *J* = 4.8 Hz, 1H), 8.08 (td, *J* = 1.8, 8.1 Hz, 1H), 8.0 (dt, *J* = 1.2, 7.8 Hz, 1H), 7.89 (d, *J* = 8.4 Hz, 1H), 7.81 (s, 1H), 7.66 (m, 2H), 7.48 (dd, *J* = 2.1, 8.7 Hz, 1H), 7.43 (s, 1H), 4.32–4.38 (m, 1H), 4.14–4.25 (m, 1H), 4.09–4.13 (m, 2H), 3.72 (s, 3H), 3.68 (s, 3H), 3.51–3.62 (m, 1H), 3.21–3.26 (m, 2H), 3.11–3.18 (m, 1H), 2.79–2.87 (m, 3H), 1.92–1.99 (m, 1H), 1.68–1.88 (m, 2H), 1.05–1.17 (m, 2H). MS *m/z* 614.4 (M + H⁺).

[[1-(3-Benzyl-3*H*-imidazol-4-ylmethyl)-6-cyano-1,2,3,4-tetrahydro-quinolin-3-yl]-[1-methyl-1*H*-imidazole-4-sulfonyl]-amino]-acetic Acid *tert*-Butyl Ester (254). ¹H NMR (300 MHz, methanol-*d*₄) δ 8.86 (s, 1H), 7.11–7.50 (m, 10 H), 6.55 (d, *J* = 8.5 Hz, 1H), 5.12 (s, 2H), 4.62–4.78 (m, 2H), 4.39–4.59 (m, 1H), 4.19 (d, *J* = 17.1 Hz, 1H), 4.0 (d, *J* = 17.1 Hz, 1H), 3.81 (s, 3H), 3.55–3.62 (m, 1H), 3.42–3.47 (m, 1H), 3.07–3.14 (m, 1H), 2.97 (m, 1H), 1.42 (s, 9H). MS *m/z* 602.2 (M + H⁺).

4-[[[6-Cyano-1-pyridin-3-ylmethyl-1,2,3,4-tetrahydro-quinolin-3-yl)-(pyridine-2-sulfonyl)-amino]-methyl]-piperidine-1-carboxylic Acid Methyl Ester (256). ¹H NMR (300 MHz, methanol-*d*₄) δ 8.84–8.89 (m, 2H), 8.70–8.75 (m, 1H), 8.49–8.51 (m, 1H), 8.03–8.19 (m, 3H), 7.68 (ddd, *J* = 1.5, 4.8, 7.5 Hz, 1H), 7.43 (d, *J* = 1.2 Hz, 1H), 7.38 (dd, *J* = 2.1, 8.7 Hz, 1H), 6.81 (d, *J* = 8.7 Hz, 1H), 4.68–4.83 (m, 2H), 4.38–4.51 (m, 1H), 4.08–4.16 (m, 2H), 3.65 (s, 3H), 3.51–3.62 (m, 2H), 3.21–3.26 (m, 2H), 3.11–3.18 (m, 1H), 2.79–2.87 (m, 3H), 1.68–1.88 (m, 3H), 1.05–1.17 (m, 2H). MS *m/z* 561.4 (M + H⁺).

General Procedure for the Synthesis of Compounds According to Scheme 6. A suspension of the aryl bromide 21 (500 mg, 1.53 mmol), phenyl boronic acid (559 mg, 4.58 mmol), and tetrakis triphenylphosphine palladium (177 mg, 10 mol %) in dimethoxyethane (15 mL) was thoroughly degassed and stirred under argon. Deionized water (3 mL) and barium hydroxide octahydrate (1.45 gm, 4.58 mmol) were added, and the reaction mixture was heated at reflux for 2 h. The reaction mixture was diluted with ethyl acetate, washed with water and brine, dried (Na₂SO₄), and concentrated under reduced pressure. The residue was purified by flash chromatography over a silica gel column to give 22 (120 mg, 45%) as a colorless solid. ¹H NMR (CDCl₃) δ 7.49 (d, *J* = 8.1 Hz, 1H), 7.36 (t, *J* = 7.8 Hz, 2H), 7.23 (t, *J* = 7.4 Hz, 4H), 6.51 (d, *J* = 8.1 Hz, 1H), 5.04 (d, *J* = 7.5 Hz, 1H), 4.11 (br s, 1H), 3.95 (s, 1H),

3.37–3.33 (m, 1H), 3.19–3.16 (m, 1H), 3.09–3.02 (m, 1H), 2.77–2.72 (m, 1H), 1.43 (s, 9H).

To a stirred solution of the phenyl derivative 22 (120 mg, 0.37 mmol) in CH₂Cl₂ (1.6 mL) at room temperature, trifluoroacetic acid (0.4 mL) was added, and the reaction mixture was stirred for 2 h. The solution was concentrated under reduced pressure, and the crude amine (trifluoroacetate salt) 23 was taken to the next step without further purification.

To a mixture of the amine 23 in CH₂Cl₂ (2 mL), diisopropyl-ethylamine (0.5 mL) was added and the reaction mixture was stirred at room temperature for 0.5 h. The appropriate sulfonyl chloride (0.37 mmol) was added, and the reaction mixture was stirred for an additional 2 h. The reaction mixture was partitioned between water and ethyl acetate. The organic layer was washed with brine, dried (Na₂SO₄), and evaporated under reduced pressure. Purification by flash chromatography gave 24 (89%) as a pale yellow solid. ¹H NMR (methanol-*d*₄) δ 7.93 (s, 1H), 7.76 (s, 1H), 7.69 (d, *J* = 1.2 Hz, 1H), 7.49 (dd, *J* = 1.2, 8.4 Hz, 2H), 7.35 (t, *J* = 7.5 Hz, 2H), 7.22 (d, *J* = 7.5 Hz, 1H), 7.11 (s, 1H), 6.60 (d, *J* = 8.4 Hz, 1H), 3.77 (s, 3H), 3.74–3.69 (m, 1H), 3.39–3.36 (m, 1H), 3.09 (dd, *J* = 8.1, 11.4 Hz, 1H), 2.93 (dd, *J* = 4.5, 15.6 Hz, 1H), 2.76 (dd, *J* = 8.1, 15.6 Hz, 1H).

To a stirred solution of the sulfonamide 24 (0.33 mmol) in dichloroethane (1 mL) and trifluoroacetic acid (1 mL) was added 3-methyl-3*H*-imidazole-4-carbaldehyde (91 mg, 0.83 mmol) at room temperature, and the reaction mixture was heated to 50 °C for 1 h. Triethylsilane (0.13 mL, 0.83 mmol) was added and stirring was continued for an additional 48 h. Volatile materials were removed under vacuum, and the reaction mixture was diluted with ethyl acetate, washed with aqueous NaHCO₃ solution, water, and brine, dried (Na₂SO₄), filtered, and concentrated in vacuum. Purification by flash chromatography afforded 25 (50 mg, 33%) as a pale yellow foam. ¹H NMR (methanol-*d*₄) δ 8.89 (s, 1H), 8.06 (s, 1H), 7.67 (s, 1H), 7.49 (t, *J* = 7.8 Hz, 3H), 7.37–7.33 (m, 3H), 7.24–7.20 (m, 2H), 6.85 (d, *J* = 7.8 Hz, 1H), 4.74 (d, *J* = 17.1 Hz, 1H), 4.57 (d, *J* = 17.1 Hz, 1H), 3.93–3.71 (m, 8H), 3.35–3.31 (m, 1H), 3.04 (dd, *J* = 4.5, 15.6 Hz, 1H), 2.76 (dd, *J* = 6.3, 15.9 Hz, 1H).

A mixture of 25 (1 equiv), Cs₂CO₃ (2 equiv), and the appropriate bromide (1 equiv) in anhydrous DMF was stirred overnight at room temperature. The reaction mixture was partitioned between water and ethyl acetate. The organic layer was washed with brine, dried (Na₂SO₄), and evaporated under reduced pressure. The crude residue was purified by HPLC.

1-Methyl-1*H*-imidazole-4-sulfonic Acid [1-(3-Methyl-3*H*-imidazol-4-ylmethyl)-6-phenyl-1,2,3,4-tetrahydro-quinolin-3-yl]-[2-pyrrol-1-yl-ethyl]-amide (272). ¹H NMR (methanol-*d*₄) δ 7.74 (d, *J* = 1.0 Hz, 1H), 7.70 (d, *J* = 1.5 Hz, 1H), 7.53 (br s, 1H), 7.52–7.50 (m, 2H), 7.39–7.33 (m, 3H), 7.26–7.22 (m, 1H), 7.17–7.16 (m, 1H), 6.90 (d, *J* = 8.5 Hz, 1H), 6.80 (br s, 1H), 6.63 (t, *J* = 2.0 Hz, 2H), 6.04 (t, *J* = 2.0 Hz, 2H), 4.44 (d, *J* = 15.5 Hz, 1H), 4.27 (d, *J* = 15.5 Hz, 1H), 4.22–4.17 (m, 4H), 3.75 (s, 3H), 3.63 (s, 3H), 3.48–3.44 (m, 2H), 2.91 (dd, *J* = 4.5, 11.5 Hz, 1H), 2.76–2.66 (m, 2H). MS *m/z* 556.3 (M + H⁺).

***N*-*tert*-Butyl-2-[(1-methyl-1*H*-imidazole-4-sulfonyl)-[1-(3-methyl-3*H*-imidazol-4-ylmethyl)-6-phenyl-1,2,3,4-tetrahydro-quinolin-3-yl]-amino]-acetamide (267).** ¹H NMR (methanol-*d*₄) δ 8.87 (s, 1H), 7.78 (d, *J* = 1.2 Hz, 2H), 7.45 (d, *J* = 7.2 Hz, 2H), 7.41 (s, 1H), 7.32 (t, *J* = 7.5 Hz, 3H), 7.19 (t, *J* = 7.2 Hz, 2H), 6.82 (d, *J* = 7.8 Hz, 1H), 4.65 (d, *J* = 15.6 Hz, 1H), 4.52 (d, *J* = 15.6 Hz, 1H), 4.36–4.18 (m, 1H), 3.94–3.75 (m, 9H), 3.31–3.40 (m, 1H), 3.02–2.85 (m, 2H), 1.31 (m, 9H). MS *m/z* 576.4 (M + H⁺).

1-Methyl-1*H*-imidazole-4-sulfonic Acid (4-Methanesulfonyl-benzyl)-[1-(3-methyl-3*H*-imidazol-4-ylmethyl)-6-phenyl-1,2,3,4-tetrahydroquinolin-3-yl]-amide (278). ¹H NMR (300 MHz, methanol-*d*₄) δ 8.87 (s, 1H), 7.92 (d, *J* = 8.4 Hz, 2H), 7.85 (s, 1H), 7.80 (s, 1H), 7.62 (d, *J* = 8.4 Hz, 2H), 7.52 (d, *J* = 8.4 Hz, 2H), 7.40–7.30 (m, 4H), 7.28–7.22 (m, 2H), 6.72 (d, *J* = 8.4 Hz, 1H), 4.75 (d, *J* = 16.5 Hz, 2H), 4.55–4.50 (m, 1H), 4.48 (d, *J* = 17.4 Hz, 1H), 4.35 (d, *J* = 16.5 Hz, 1H), 3.85 (s, 3H), 3.80 (s, 3H), 3.42–3.36 (m, 2H), 3.12 (s, 3H), 3.08–2.95 (m, 2H). MS *m/z* 631.6 (M + H⁺).

1-Methyl-1*H*-imidazole-4-sulfonic Acid (2-Bromo-allyl)-[1-(3-methyl-3*H*-imidazol-4-ylmethyl)-6-phenyl-1,2,3,4-tetrahydroquinolin-3-yl]-amide (264). ¹H NMR (300 MHz, methanol-*d*₄) δ 8.92 (s, 1H), 7.80 (d, *J* = 3.9 Hz, 2H), 7.55 (dd, *J* = 1.2, 8.4 Hz, 2H), 7.45 (s, 1H), 7.40 (t, *J* = 8.7 Hz, 3H), 7.32–7.20 (m, 2H), 6.90 (d, *J* = 8.7 Hz, 1H), 6.10 (d, *J* = 2.1 Hz, 1H), 5.65 (d, *J* = 2.1 Hz, 1H), 4.75 (d, *J* = 16.8 Hz, 1H), 4.60 (d, *J* = 17.1 Hz, 1H), 4.50–4.40 (m, 1H), 4.20 (d, *J* = 18.0 Hz, 1H), 4.10 (d, *J* = 18.0 Hz, 1H), 3.95 (s, 3H), 3.80 (s, 3H), 3.49–3.40 (m, 2H), 3.15–3.05 (m, 1H), 2.87 (dd, *J* = 5.1, 15.6 Hz, 1H). MS *m/z* 583.0 (M + H⁺).

1-Methyl-1*H*-imidazole-4-sulfonic Acid Ethyl-[1-(3-methyl-3*H*-imidazol-4-ylmethyl)-6-phenyl-1,2,3,4-tetrahydroquinolin-3-yl]amide (259). ¹H NMR (300 MHz, methanol-*d*₄) δ 8.90 (s, 1H), 7.75 (s, 1H), 7.72 (s, 1H), 7.52 (dd, *J* = 1.2, 8.7 Hz, 2H), 7.45 (s, 1H), 7.35 (t, *J* = 7.2 Hz, 3H), 7.30–7.20 (m, 2H), 6.87 (d, *J* = 8.7 Hz, 1H), 4.75 (d, *J* = 16.8 Hz, 1H), 4.57 (d, *J* = 16.8 Hz, 1H), 4.47–4.37 (m, 1H), 3.95 (s, 3H), 3.80 (s, 3H), 3.45–3.25 (m, 4H), 3.20–3.10 (m, 1H), 2.90 (m, 1H), 1.25 (t, *J* = 6.9 Hz, 3H). MS *m/z* 491.5 (M + H⁺).

{1-(1-Methyl-1*H*-imidazole-4-sulfonyl)-[1-(3-methyl-3*H*-imidazol-4-ylmethyl)-6-phenyl-1,2,3,4-tetrahydroquinolin-3-yl]-amino}-acetic Acid Methyl Ester (266). ¹H NMR (300 MHz, methanol-*d*₄) δ 8.92 (s, 1H), 7.80 (s, 1H), 7.75 (s, 1H), 7.52 (dd, *J* = 1.2, 8.4 Hz, 2H), 7.44 (s, 1H), 7.36 (t, *J* = 7.5 Hz, 3H), 7.30–7.25 (m, 2H), 6.85 (d, *J* = 8.7 Hz, 1H), 4.75 (d, *J* = 16.8 Hz, 1H), 4.55 (d, *J* = 16.8 Hz, 1H), 4.50–4.40 (m, 1H), 4.15 (d, *J* = 18.3 Hz, 1H), 4.08 (d, *J* = 18.6 Hz, 1H), 3.95 (s, 3H), 3.80 (s, 3H), 3.70 (s, 3H), 3.55–3.45 (m, 2H), 3.05–2.90 (m, 2H). MS *m/z* 535.4 (M + H⁺).

General Procedure for the Synthesis of Compounds According to Scheme 7. General Procedure for the Conversion of Nitrile (5) to Amide (28). To a stirred solution of nitrile **5** (441 mg, 1 mmol) in alcohol (8 mL) was slowly added concentrated sulfuric acid (0.05 mL) at room temperature. The resulting solution was stirred at 40 °C for 2 h. The mixture was poured into cold aqueous 20% KHCO₃ solution to neutralize the acid and precipitate the product. The product was filtered, washed with cold water, and dried under vacuum to give amides **28** (40–45%).

3-(1-Methyl-1*H*-imidazole-4-sulfonylamino)-1-(3-methyl-3*H*-imidazol-4-ylmethyl)-1,2,3,4-tetrahydroquinoline-6-carboxylic Acid *tert*-Butylamide (28). ¹H NMR (300 MHz, methanol-*d*₄) δ 8.90 (s, 1H), 7.80 (s, 1H), 7.70 (s, 1H), 7.51 (dd, *J* = 2.1, 8.7 Hz, 1H), 7.45 (s, 1H), 7.40 (d, *J* = 2.1 Hz, 1H), 6.80 (d, *J* = 8.7 Hz, 1H), 4.80 (d, *J* = 16.8 Hz, 1H), 4.60 (d, *J* = 16.8 Hz, 1H), 3.92 (s, 3H), 3.86–3.83 (m, 1H), 3.80 (s, 1H), 3.52–3.45 (m, 1H), 3.42–3.35 (m, 1H), 3.0 (dd, *J* = 4.8, 16.5 Hz, 1H), 2.74 (dd, *J* = 6.3, 16.2 Hz, 1H), 1.45 (s, 9H). MS *m/z* 486.4 (M + H⁺).

3-[(*tert*-Butylcarbamoyl-methyl)-(1-methyl-1*H*-imidazol-4-sulfonyl)-amino]-1-(3-methyl-3*H*-imidazol-4-ylmethyl)-1,2,3,4-tetrahydroquinolin-6-carboxylic Acid *tert*-Butylamide (285). The compound was prepared using the general *N*-alkylation procedure (**5** to **2**, Scheme 1). ¹H NMR (300 MHz, methanol-*d*₄) δ 8.92 (s, 1H), 7.85 (s, 1H), 7.80 (s, 1H), 7.52 (dd, *J* = 2.1, 8.7 Hz, 1H), 7.43 (s, 1H), 7.40 (d, *J* = 2.1 Hz, 1H), 6.79 (d, *J* = 8.7 Hz, 1H), 4.75 (d, *J* = 16.8 Hz, 1H), 4.63 (d, *J* = 16.8 Hz, 1H), 4.33–4.25 (m, 1H), 3.92 (s, 3H), 3.87 (s, 2H), 3.81 (s, 3H), 3.57–3.51 (m, 1H), 3.44–3.40 (m, 1H), 3.03 (dd, *J* = 4.5, 15.9 Hz, 1H), 2.80 (dd, *J* = 4.5, 15.9 Hz, 1H), 1.43 (s, 9H), 1.35 (s, 9H). MS *m/z* 599.5 (M + H⁺).

General Procedure for the Conversion of Nitrile (5) to Acid (27). A solution of **5** (441 mg, 1.0 mmol) in concentrated HCl (20 mL) was stirred at 80 °C for 2 h. The reaction mixture was cooled to room temperature and then evaporated to dryness under reduced pressure. The residue was dissolved in saturated LiOH solution (pH 9) and then evaporated to dryness under reduced pressure. The residue was dissolved in 10% aqueous HCl solution (pH 2), evaporated, and dried under vacuum to give the corresponding acid **27**, which was used in the next step without further purification. ¹H NMR (300 MHz, methanol-*d*₄) δ 8.90 (s, 1H), 7.80 (s, 1H), 7.70 (s, 1H), 7.62 (dd, *J* = 2.1, 8.7 Hz, 1H), 7.52 (d, *J* = 2.1 Hz, 1H), 7.42 (s, 1H), 6.80 (d, *J* = 8.7 Hz, 1H), 4.80 (d, *J* = 16.8 Hz,

1H), 4.62 (d, *J* = 16.8 Hz, 1H), 3.92 (s, 3H), 3.90–3.82 (m, 1H), 3.80 (s, 3H), 3.55–3.45 (m, 1H), 3.43–3.38 (m, 1H), 3.03 (dd, *J* = 4.8, 16.5 Hz, 1H), 2.76 (dd, *J* = 6.3, 16.2 Hz, 1H). MS *m/z* 486.4 (M + H⁺).

To a mixture of the acid **27** (430 mg, 1.0 mmol) above, benzyl amine (107 mg, 1 mmol), and *N,N*-dimethylamino pyridine (18 mg, 0.15 mmol) in DMF was added EDC (287 mg, 1.5 mmol), and the mixture was stirred at room temperature for 20 h. The mixture was concentrated under reduced pressure, and aqueous NaHCO₃ solution (20 mL) was added. The mixture was extracted with 10% MeOH in CHCl₃ (3 × 30 mL), and the organic layer was dried (Na₂SO₄) and evaporated under reduced pressure. The crude product was purified by flash chromatography to afford **28** (220 mg, 38%).

3-(1-Methyl-1*H*-imidazole-4-sulfonylamino)-1-(3-methyl-3*H*-imidazol-4-ylmethyl)-1,2,3,4-tetrahydroquinoline-6-carboxylic Acid Benzylamide (28). ¹H NMR (300 MHz, methanol-*d*₄) δ 8.90 (s, 1H), 7.76 (s, 1H), 7.70 (s, 1H), 7.62 (dd, *J* = 2.1, 8.7 Hz, 1H), 7.50 (d, *J* = 2.1 Hz, 1H), 7.46 (s, 1H), 7.36–7.30 (m, 5H), 6.82 (d, *J* = 8.7 Hz, 1H), 4.75 (d, *J* = 16.8 Hz, 1H), 4.62 (d, *J* = 16.8 Hz, 1H), 4.55 (s, 2H), 3.92 (s, 3H), 3.90–3.82 (m, 1H), 3.80 (s, 3H), 3.53–3.48 (m, 1H), 3.43–3.39 (m, 1H), 3.03 (dd, *J* = 4.8, 16.5 Hz, 1H), 2.75 (dd, *J* = 6.3, 16.2 Hz, 1H).

3-[(*tert*-Butylcarbamoyl-methyl)-(1-methyl-1*H*-imidazol-4-sulfonyl)-amino]-1-(3-methyl-3*H*-imidazol-4-ylmethyl)-1,2,3,4-tetrahydroquinolin-6-carboxylic Acid Benzylamide (291). Compound **291** was prepared as described from the general procedure for *N*-alkylation. ¹H NMR (300 MHz, methanol-*d*₄) δ 8.92 (s, 1H), 7.80 (s, 1H), 7.78 (s, 1H), 7.63 (dd, *J* = 2.1, 8.7 Hz, 1H), 7.53 (d, *J* = 2.1 Hz, 1H), 7.42 (s, 1H), 7.36–7.30 (m, 5H), 6.82 (d, *J* = 8.7 Hz, 1H), 4.77 (d, *J* = 16.8 Hz, 1H), 4.65 (d, *J* = 17.4 Hz, 1H), 4.55 (s, 2H), 4.33–4.22 (m, 1H), 3.91 (s, 3H), 3.85 (s, 2H), 3.80 (s, 3H), 3.56–3.50 (m, 1H), 3.46–3.39 (m, 1H), 3.03 (dd, *J* = 5.1, 15.3 Hz, 1H), 2.86 (dd, *J* = 5.1, 15.3 Hz, 1H), 1.4 (s, 9H). MS *m/z* 633.8 (M + H⁺).

3-[(*tert*-Butylcarbamoyl-methyl)-(1-methyl-1*H*-imidazol-4-sulfonyl)-amino]-1-(3-methyl-3*H*-imidazol-4-ylmethyl)-1,2,3,4-tetrahydroquinolin-6-carboxylic Acid (289). Compound **289** was prepared as described from general procedure for *N*-alkylation. ¹H NMR (300 MHz, methanol-*d*₄) δ 8.92 (s, 1H), 7.82 (s, 1H), 7.79 (s, 1H), 7.62 (dd, *J* = 2.1, 8.7 Hz, 1H), 7.52 (d, *J* = 2.1 Hz, 1H), 7.42 (s, 1H), 6.80 (d, *J* = 8.7 Hz, 1H), 4.75 (d, *J* = 16.8 Hz, 1H), 4.65 (d, *J* = 16.8 Hz, 1H), 4.35–4.25 (m, 1H), 3.92 (s, 3H), 3.85 (s, 2H), 3.80 (s, 3H), 3.60–3.51 (m, 1H), 3.50–3.40 (m, 1H), 3.03 (dd, *J* = 4.8, 16.5 Hz, 1H), 2.80 (dd, *J* = 6.3, 16.2 Hz, 1H), 1.40 (s, 9H). MS *m/z* 543.5 (M + H⁺).

Synthesis of 34 According to Scheme 8. Preparation of 1-[4-(*N*-triphenylmethyl)imidazolyl]ethanol. To an ice-bath cooled solution of 3.35 mL (10.0 mmol) of 3 M methyl magnesium bromide in 40 mL dry ether was added a solution of 4-(*N*-triphenylmethyl)imidazole carboxaldehyde (1.69 g, 10 mmol) in THF. After 1.5 h at ambient temperature, a concentrated solution of 0.67 g (25 mmol) NH₄Cl in water was added to the reaction mixture. The mixture was stirred for 1 h and filtered, and the solids were washed with THF. The combined filtrate and washes were washed with water and brine, dried over Na₂SO₄, and concentrated in vacuo to afford the required compound.¹⁷ ¹H NMR (300 MHz CDCl₃) 7.42 (s, 1H), 7.30–7.39 (m, 9H), 7.10–7.21 (m, 6H), 6.85 (s, 1H), 4.85 (q, 1H), 1.5 (d, 3H). MS *m/z* 355.2 (M + H⁺).

A mixture of **33** (47 mg, 0.1 mmol) and 1-(4-(*N*-triphenylmethyl)imidazolyl)ethanol (17 mg, 0.05 mmol) in 5 mL of dry acetonitrile was added methanesulfonyl chloride (34 mg, 0.3 mmol), and the mixture was heated at 60 °C overnight under nitrogen. Aqueous NaHCO₃ and ethyl acetate were added. The organic layer was washed with water and brine and dried over MgSO₄. The crude product was purified by HPLC to give **34** as a mixture of isomers.¹⁸ ¹H NMR (300 MHz, methanol-*d*₄) δ 8.95 (s, 1H), 8.94 (s, 1H), 8.72 (d, *J* = 7.5 Hz, 1H), 8.68 (d, *J* = 7.5 Hz, 1H), 7.90–8.10 (m, 4H), 7.59–7.70 (m, 4H), 7.31–7.48 (m, 4H), 6.95 (d, *J* = 8.7 Hz, 1H), 6.91 (d, *J* = 8.7 Hz, 1H), 5.50 (q, 1H), 5.40 (q, 1H), 4.38–4.51 (m, 2H), 4.08–4.16 (m, 4H), 3.70 (s, 6H), 3.32–3.45 (m,

4H), 3.01–3.22 (m, 6H), 2.65–2.90 (m, 6H), 1.68–1.88 (m, 6H), 1.60 (d, 6H), 1.05–1.17 (m, 4H). MS m/z 564.6 (M + H⁺).

Resolution of Enantiomers (163 and 164). Enantiomerically pure amines derived from racemic 6-cyano-1,2,3,4-tetrahydroquinolin-3-ylamine hydrochloride were obtained by coupling with *S*-mandelic acid to form diastereomeric amides as described previously.^{5,10} After resolution, the amines were converted to **163** and **164**, as shown in Scheme 1.

Modeling Studies. We published a detailed procedure for building a homology model of Pf-PFT.⁷ Briefly, the model was generated with MODELLER¹⁹ by using the crystal structure of rat-PFT complexed with the nonsubstrate tetrapeptide inhibitor CVFM and farnesyl-pyrophosphate as the template structure (PDB entry 1JCR). The sequences of the two subunits (α and β) of Pf-PFT were obtained from the PlasmoDB²⁰ (α : PFL2050w and β : chr11.glm_528) and aligned with the template. Only regions with reasonable reliability in the alignment were included. The model of Pf-PFT comprises the following sequence segments (the residue numbers of the corresponding segments of the rat-PFT subunits are given in parentheses): α : 72–164 (87–179), 300–411 (184–283); β : 421–677 (71–315), 806–896 (330–417). Note that the Pf-PFT sequences (α : 497; β : 967) are much longer than the rat ones (α : 377; β : 437).

A small molecule crystal structure of 7-nitro-1,2,3,4-THQ,²¹ with $R = 0.034$ at 0.77 Å resolution, shows that the tetrahydropyridine ring adopts an envelope conformation, with atom C3 deviating by 0.66 Å from the mean plane through the other five atoms. Upon substitution with an equatorial amino group, the deviation of the methyl from the plane is 0.40 Å, implying that when the two enantiomers are superimposed the amines are only 0.40 Å apart. Both conformers of the molecule were built with Insight (Accelrys) starting from the 7-nitro-1,2,3,4-THQ crystal structure, and the energies were minimized with the CFF force-field; a 4re electrostatics model was used. The energies were 54.28 kcal/mol (equatorial) and 56.96 kcal/mol (axial).

All molecular docking calculations of the THQ compounds were carried out using the FLO/QXP v.6.02 package²⁴ with as start model **162**, as observed in the rat-PFT crystal structure transferred by superposition into the comparative model of Pf-PFT. THQ compounds were built with the FLO BUILDER module, specifically taking care to assign the mixed sp²/sp³ N atom type of the sulfonamide and allowing for mild pyramidalization. Monte Carlo searches were carried out for the THQ substituents, using 50 cycles per rotatable bond, while keeping the THQ scaffold fixed. Subsequently, the best solutions were minimized, allowing also for spatial freedom to the scaffold. Because the force-field has not been parametrized for transition metal complexes, the inhibitor N atom that coordinates the Zn²⁺ atom was spatially constrained as well as all other atoms of the Zn²⁺-binding imidazole ring.

Plasmodium Strains. The *P. falciparum* strains used in this study were 3D7 (Netherlands [airport-associated malaria], chloroquine sensitive) and K1 (Thailand, chloroquine resistant, pyrimethamine resistant). Strain 3D7 was provided by Dr. Pradipsinh Rathod from the University of Washington. *P. falciparum* strain K1 and *P. berghei* isolate NK65 (used for rodent malaria experiments) were obtained from the MR4 unit of the American Type Culture Collection (ATCC, Manassas, VA).

***P. falciparum* Culture.** Strains of *P. falciparum* were cultured in vitro using experimental techniques described by Trager and Jensen.²² Cultures were maintained in RPMI-1640 (Sigma, St. Louis, MI) with 2 mM L-glutamine, 25 mM HEPES, 33 mM NaHCO₃, 20 μg/mL gentamicin sulfate, and 20% (v/v) heat-inactivated human plasma type A+ (RP-20P). Type A+ erythrocytes were obtained from lab donors, washed three times with RPMI 1640, resuspended in 50% RPMI-1640, and stored at 4 °C. Parasites were grown in 10 mL of a 2% hematocrit/RP-20P (v/v) in 50 mL flasks under a 5% CO₂, 5% O₂, and 90% N₂ atmosphere.

***P. falciparum* ED₅₀ Determination.** A total of 10 μL of PFTI in solution was added to each well of a 96-well plate followed by the addition of 190 μL of an asynchronous *P. falciparum* culture at parasitemia and hematocrit of 0.5%. PFTI solutions were prepared

by diluting 20 mM THQ PFTI in dimethylsulfoxide by 200-fold with RP-20P for the highest concentration (100 μM stock gives final assay concentration of 5 μM), then performing further serial dilutions in RP-20P. Plates were flushed with 5% CO₂, 5% O₂, and 90% N₂ then incubated at 37 °C for 48 h. 8[³H]-Hypoxanthine (0.3 μCi, 20 Ci/mmol, American Radiolabeled Chemicals) in 30 μL of RP-20P was added to cultures and incubated for an additional 24 h. Cells were harvested onto glass fiber filters by a cell harvester (Inotech Biosystems International, Inc Rockville, MD), and the radioactivity incorporated into the parasites was counted on a Chameleon 425-104 multilabel plate counter (Hidex Oy Turku, Finland). The background level detected with uninfected erythrocytes was subtracted from the data. The ³H-incorporation into infected erythrocytes with 1 μL of DMSO vehicle alone represents 100% malaria growth. ED₅₀ values, the effective dose that reduces growth by 50%, were determined by linear regression analysis of the plots of ³H-hypoxanthine incorporation versus concentration of compound. Each compound was tested in duplicate, and the mean value is shown; individual measurements differed by less than 3-fold.

Pf-PFT IC₅₀ Determination. The PFT assay used to determine the IC₅₀s (inhibitor concentration that causes 50% enzyme inhibition) of the compounds is based on a PFT [³H] scintillation proximity assay (SPA; TRKQ7010 Amersham Biosciences Corp Piscataway, NJ).³ Assays were carried out in assay buffer (pH 7.5, 50 mM HEPES, 30 mM MgCl₂, 20 mM KCl, 5 mM DTT, 0.01% Triton X-100), 1 μM human lamin-B carboxy-terminus sequence peptide (biotin-YRASNRSICAIM), and 1 μCi ³H-farnesylpyrophosphate (Amersham specific activity 15 to 20 Ci/mM) in a total volume of 50 μL, which included 1 μL of Pf-PFT inhibitor solution in DMSO and 5 μL of partially purified Pf-PFT. Assays in the absence of Pf-PFT inhibitor and Pf-PFT were included as positive and negative controls, respectively. Reaction mixtures were incubated at 37 °C for 60 min and terminated by the addition of 70 μL of assay STOP solution and 5 μL of SPA beads. The assay mixture was incubated at room temperature for 30 min. The assay was counted on a plate Chameleon 425-104 multilabel counter (Hidex Oy Turku, Finland). IC₅₀ values were calculated using linear regression analysis of the plots of the amount of radio-prenylation versus the concentration of compound.

Mammalian-PFT IC₅₀ Determination. The PFT assay used to determine the IC₅₀s of the compounds is based on a farnesyl transferase [³H] SPA enzyme assay (TRKQ7010 Amersham Biosciences Corp Piscataway, NJ). Rat PFT was prepared as described.²³ Assays were carried out in assay buffer pH 7.5 (50 mM HEPES, 30 mM MgCl₂, 20 mM KCl, 5 mM DTT, 0.01% Triton X-100) and 1 μM human lamin-B carboxy-terminus sequence peptide (biotin-YRASNRSICAIM) in a total volume of 50 μL, which included 1 μL of PFT inhibitor solution in DMSO and 5 μL of partially purified rat-PFT. Assays in the absence of PFT inhibitor and rat-PFT were included as positive and negative controls, respectively. Reaction mixtures were incubated at 37 °C for 15 min and terminated by the addition of 70 μL of assay STOP solution and 5 μL of SPA beads. The assay is incubated at room temperature for 30 min. The assay was counted on a plate Chameleon 425-104 multilabel counter (Hidex Oy Turku, Finland). IC₅₀ values were calculated using linear regression analysis of the plots of ³H-FPP prenylation versus concentration of compounds.

Note Added after ASAP Publication. This manuscript was released ASAP on August 28, 2007, with errors in the compound numbers in Schemes 5 and 7 and with an error in the structure for compound **119** in Table 2. The correct version was posted on September 13, 2007.

Supporting Information Available: HPLC traces of key compounds **6**, **162**, **110**, **191**, and **234**. This material is available free of charge via the Internet at <http://pubs.acs.org>.

References

- (1) Chakrabarti, D.; Azam, T.; DelVecchio, C.; Qiu, L.; Park, Y.; Allen, C. M. Protein prenyl transferase activities of *Plasmodium falciparum*. *Mol. Biochem. Parasitol.* **1998**, *94*, 175–184.
- (2) Chakrabarti, D.; Da Silva, T.; Barger, J.; Paquette, S.; Patel, H.; Patterson, S.; Allen, C. M. Protein farnesyltransferase and protein prenylation in *Plasmodium falciparum*. *J. Biol. Chem.* **2002**, *277*, 42066–42073.
- (3) Nallan, L.; Bauer, K. D.; Bendale, P.; Rivas, K.; Yokoyama, K.; Horney, C. P.; Pandyala, P. R.; Floyd, D.; Lombardo, L. J.; Williams, D. K.; Hamilton, A.; Sehti, S.; Windsor, W. T.; Weber, P. C.; Buckner, F. S.; Chakrabarti, D.; Gelb, M. H.; Van Voorhis, W. C. Protein farnesyltransferase inhibitors exhibit potent antimalarial activity. *J. Med. Chem.* **2005**, *48*, 3704–3713.
- (4) Bell, I. M. Inhibitors of farnesyltransferase: A rational approach to cancer chemotherapy? *J. Med. Chem.* **2004**, *47*, 1869–1878.
- (5) Lombardo, L. J.; Camuso, A.; Clark, J.; Fager, K.; Gullo-Brown, J.; Hunt, J. T.; Inigo, I.; Kan, D.; Koplowitz, B.; Lee, F.; McGlinchey, K.; Qian, L.; Ricca, C.; Rovnyak, G.; Traeger, S.; Tokarski, J.; Williams, D. K.; Wu, L. I.; Zhao, Y.; Manne, V.; Bhide, R. S. Design, synthesis, and structure–activity relationships of tetrahydroquinoline-based farnesyltransferase inhibitors. *Bioorg. Med. Chem. Lett.* **2005**, *15*, 1895–1899.
- (6) Hunt, J. T.; Ding, C. Z.; Batorsky, R.; Bednarz, M.; Bhide, R.; Cho, Y.; Chong, S.; Chao, S.; Gullo-Brown, J.; Guo, P.; Kim, S. H.; Lee, F. Y.; Leftheris, K.; Miller, A.; Mitt, T.; Patel, M.; Penhallow, B. A.; Ricca, C.; Rose, W. C.; Schmidt, R.; Slusarchyk, W. A.; Vite, G.; Manne, V. Discovery of (*R*)-7-cyano-2,3,4,5-tetrahydro-1-(1*H*-imidazol-4-ylmethyl)-3-phenylmethyl-4-(2-thienylsulfonyl)-1*H*-1,4-benzodiazepine (BMS-214662), a farnesyltransferase inhibitor with potent preclinical antitumor activity. *J. Med. Chem.* **2000**, *43*, 3587–3595.
- (7) Eastman, R. T.; White, J.; Hucke, O.; Bauer, K.; Yokoyama, K.; Nallan, L.; Chakrabarti, D.; Verlinde, C. L.; Gelb, M. H.; Rathod, P. K.; Van Voorhis, W. C. Resistance to a protein farnesyltransferase inhibitor in *Plasmodium falciparum*. *J. Biol. Chem.* **2005**, *280*, 13554–13559.
- (8) Eastman, R. T.; White, J.; Hucke, O.; Yokoyama, K.; Verlinde, C. L.; Hast, M. A.; Beese, L. S.; Gelb, M. H.; Rathod, P. K.; Van Voorhis, W. C. Resistance mutations at the lipid substrate binding site of *Plasmodium falciparum* protein farnesyltransferase. *Mol. Biochem. Parasitol.* **2007**, *152* (1), 66–71.
- (9) Van Voorhis, W. C.; Rivas, K.; Bendale, P.; Nallan, L.; Hornéy, C.; Barrett, L. K.; Ankala, S.; Hucke, O.; Verlinde, C. L. M. J.; Chakrabarti, D.; Strickland, C.; Yokoyama, K.; Buckner, F. S.; Hamilton, A.; Williams, D. K.; Lombardo, L. J.; Floyd, D.; Gelb, M. H. Tetrahydroquinoline *Plasmodium falciparum* protein farnesyltransferase inhibitors: Efficacy, pharmacokinetics, and metabolism. *Antimicrob. Agents Chemother.* **2007**, in press.
- (10) Bhide, R. Inhibitors of farnesyl protein transferase. WO 99/01434, 1999.
- (11) Reid, T. S.; Beese, L. S. Crystal structures of the anticancer clinical candidates R115777 (Tipifarnib) and BMS-214662 complexed with protein farnesyltransferase suggest a mechanism of FTI selectivity. *Biochemistry* **2004**, *43*, 6877–6884.
- (12) Nicholas, J. B.; Vance, R. E. M.; Burke, B. J.; Hopfinger, A. J. A molecular mechanics valence force field for sulfonamides derived by ab initio methods. *J. Chem. Phys.* **1991**, *95*, 9803–9811.
- (13) Liang, G. Y.; Bays, J. P.; Bowen, J. P. Ab initio calculations and molecular mechanics (MM3) force field development for sulfonamide and its alkyl derivatives. *Theochem.* **1997**, *40*, 1/2, 165–179.
- (14) Hillal, S. H.; Karickhoff, S. W.; Carreira, L. A. A rigorous test for SPARC's chemical reactivity models: Estimation of more than 4300 ionization p*K*(a)s. *Quant. Struct.-Act. Relat.* **1995**, *14*, 348.
- (15) Hillal, S. H.; El-Shabrawy, Y.; Carreira, L. A.; Karickhoff, W. W.; Toubar, S. S.; Rizk, M. Estimation of the ionization p*K*_a of pharmaceutical substances using the computer program sparc. *Talanta* **1996**, *43*, 607–619.
- (16) Chen, B. C.; Skoumbourdis, A. P.; Sundenen, J. E.; Rovnyak, G. C.; Traeger, S. C. Efficient molar-scale synthesis of 1-methyl-5-acylimidazole triflic acid salts. *Org. Process Res. Dev.* **2000**, *4*, 513–614.
- (17) Kelley, J. L.; Miller, C. A.; McLean, E. W. Attempted inhibition of histidine decarboxylase with β-alkyl analogues of histidine. *J. Med. Chem.* **1977**, *20*, 721–723.
- (18) Venishi, J.; Hamada, M.; Aburatani, S.; Matsui, K.; Yonemitsu, O.; Tsukube, H. Synthesis of chiral nonracemic 1-(2-pyridinyl)ethylamines: Stereospecific introduction of amino function onto the 2-pyridinylmethyl carbon center. *J. Org. Chem.* **2004**, *69*, 6781–6789.
- (19) Sali, A.; Blundell, T. L. Comparative protein modelling by satisfaction of spatial restraints. *J. Mol. Biol.* **1993**, *234*, 779–815.
- (20) Bahl, A.; Brunk, B.; Crabtree, J.; Fraunholz, M. J.; Gajria, B.; Grant, G. R.; Ginsburg, H.; Gupta, D.; Kissinger, J. C.; Labo, P.; Li, L.; Mailman, M. D.; Milgram, A. J.; Pearson, D. S.; Roos, D. S.; Schug, J.; Stoeckert, C. J., Jr.; Whetzel, P. PlasmoDB: The *Plasmodium* genome resource. A database integrating experimental and computational data. *Nucleic Acids Res.* **2003**, *31*, 212–215.
- (21) Gu, J. M.; Hu, X. R.; Xu, W. M. 7-Nitro-1,2,3,4-tetrahydroquinoline. *Acta Crystallogr.* **2006**, *E62*, o62–o63.
- (22) Trager, W.; Jensen, J. B. Human malaria parasites in continuous culture. *Science* **1976**, *193*, 673–675.
- (23) Yokoyama, K.; Zimmerman, K.; Scholten, J.; Gelb, M. H. Differential prenyl pyrophosphate binding to mammalian protein geranylgeranyltransferase-I and protein farnesyltransferase and its consequence on the specificity of protein prenylation. *J. Biol. Chem.* **1997**, *272*, 3944–3952.
- (24) McMartin, C.; Bohacek, R. S. QXP: Powerful, rapid computer algorithms for structure-based drug design. *J. Comput.-Aided Mol. Des.* **1997**, *11*, 333–344.

JM0703340